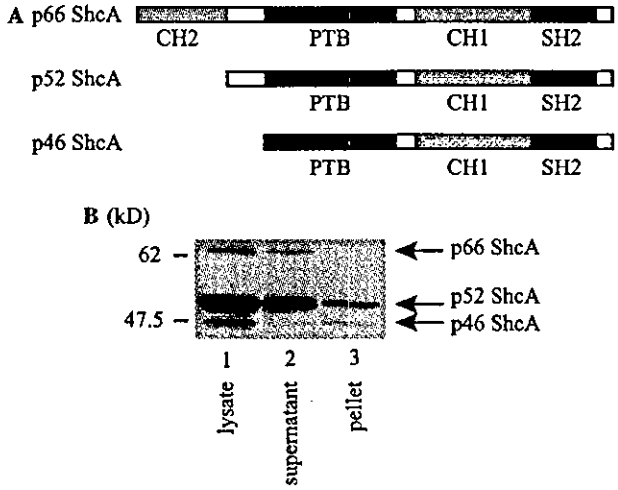

Fig. 1. ShcA is present in platelet cytosol. (A) Domain structures of p46, p52, and p66 ShcA isoforms are shown schematically. (B) Low speed supernatant of sonicated platelets (lane 1) was centrifuged at 4 °C for 30 min at 300,000*g*, and the comparable amounts of the supernatant (lane 2) and the pellet (lane 3) were analyzed by immunoblot with anti-ShcA antibody as described in the Experimental procedures. The data shown are the representative of three independent experiments with similar results.

of mice with mutations on both tyrosine residues of β_3-tail, ShcA does not undergo aggregation-induced tyrosine-phosphorylation [7]. These results suggest that ShcA may be involved in the regulation of platelet aggregation. However, it remains open whether ShcA regulates platelet aggregation.

Here, we show that ShcA binds to the tyrosine-phosphorylated β_3 peptide through its PTB domain. Exogenous addition of cytosol is required for reconstitution of aggregation of permeabilized platelets in our previously established assay [12]. Using this assay, we directly demonstrate the involvement of ShcA in the regulation of platelet aggregation by showing that the aggregation-supporting activity of the added cytosol was abolished by immunodepletion of ShcA, which was rescued by addition of recombinant ShcA.

Experimental procedures

Materials. The cDNA encoding p52 ShcA was generated by polymerase chain reaction (PCR) using Marathone cDNA of human bone marrow (Clontech) as a template and cloned into pGEX-2T (Amersham–Pharmacia) at the *Eco*RI site. The PTB (47–208) and SH2 (377–456) domains of p52 ShcA (PTB-ShcA and SH2-ShcA, respectively) were also generated by PCR with full length ShcA DNA as a template and cloned at the *Eco*RI site and the *Bam*HI–*Eco*RI site, respectively. Glutathione *S*-transferase (GST)-fusion proteins of ShcA, PTB-ShcA, and SH2-ShcA were produced in *Escherichia coli* strain BL21 and affinity-purified using glutathione–Sepharose (Amersham–Pharmacia). cDNA encoding p52 ShcA was also cloned in pDEST (Invitrogen) and p52 ShcA was produced and purified as a GST-fusion protein in Sf9 insect cells using a Bac-to-Bac system (Invitrogen). The biotinylated β_3 cytoplasmic peptides (735–762) with or without tyrosine-phosphorylation at 747 and 759 were produced by Sawady Technology, Tokyo, Japan. They were biotin-ARAKWDTANNPLYKEATSTFTNITYRGT and biotin-ARAKWDTANNPLphospho-YKEATSTFTNITphospho-YRGT. The streptoavidin–agarose, glutathione–Sepharose, and protein A–agarose were purchased from Sigma, Amersham–Pharmacia, and Roche, respectively. Anti-ShcA rabbit polyclonal and anti-GST (B-14) mouse monoclonal antibodies were purchased from BD-Transduction Laboratories and Santa Cruz Biotechnology, respectively. Horseradish peroxidase-labeled anti-rabbit and anti-mouse IgG polyclonal antibodies were from Amersham–Pharmacia, which were used as secondary antibodies for immunoblotting visualized by enhanced chemiluminescence method (Amersham). Unless otherwise specified, all the chemicals were purchased from Sigma, except for streptolysin-O (SLO), that was from Dr. S. Bhakdi, Mainz Univ., Mainz, Germany [13]. Supernatant of sonicated platelets after centrifuged at 100,000*g* for 60 min at 4 °C was used as the human platelet cytosol. All the recombinant proteins and platelet cytosol were dialyzed against Buffer A (50 mM Hepes–KOH, pH 7.4, 78 mM KCl, 4 mM $MgCl_2$, 0.2 mM $CaCl_2$, 2 mM EGTA, 1 mM dithiothreitol, and the calculated free $[Ca^{2+}]$ was approximately 20 nM [14]) and stored at −80 °C until use. The DNA sequences of all the PCR products were confirmed by DNA-sequencing using ABI PRIZM, 310 Genetic Analizer (Applied Biosystems).

The peptide affinity chromatography. The streptoavidin-coated beads (100 μl) were first incubated in Buffer A containing 0.1% Triton X-100, 1 mM Na_3VO_4, and 20 mM NaF at 4 °C for 30 min with 30 nmol of biotin and the biotin-tagged β_3 peptides. Then, the beads were washed with the same buffer and incubated at 4 °C for 3 h with the human platelet cytosol (8 mg of proteins) in the experiments for Fig. 2A, or with GST-ShcA, GST-PTB-ShcA, GST-SH2-ShcA, and GST (100 pmol) in the presence of 0.4 mg/ml BSA for Fig. 2B. Then, the beads were washed 5 times with the same buffer and added with the SDS-containing Laemmli's buffer for immunoblot analysis [15].

The aggregation assay using permeabilized platelets. The method of the aggregation assay was previously described [12], where platelets permeabilized with SLO were stimulated by $[Ca^{2+}]$ at 20 μM [14] in the presence of exogenous cytosol and an ATP regeneration system, and the light transmission was monitored.

Results and discussion

The adaptor protein ShcA consists of three isoforms with molecular weights of 66, 52, and 46 kDa which are produced by RNA splicing or alternative translational initiation [9,16,17]. All of these ShcA isoforms contain two phosphotyrosine-binding domains, PTB and SH2, and collagen homology domain 1 (CH1) (Fig. 1A) [8]. Among ShcA isoforms, p52 ShcA was predominant, and p46 and p66 ShcA were minor in platelets (Fig. 1B). Most of p52 ShcA was recovered in the supernatant after high-speed centrifugation of the sonicated platelets (Fig. 1B), indicating that p52 ShcA exists mainly in the cytosol in resting platelets.

First, to examine whether p52 ShcA could bind to β_3-tail in vitro, we incubated platelet cytosol with streptoavidin-beads coated with the biotinylated tyrosine-phosphorylated β_3-tail peptide (735–762) and the non-phosphorylated peptide. p52 ShcA was detected on the tyrosine-phosphorylated peptide-coated beads, but not on the non-phosphorylated peptide-coated beads (Fig. 2A). Then, we examined which phosphotyrosine-binding motif of ShcA, namely PTB or SH2

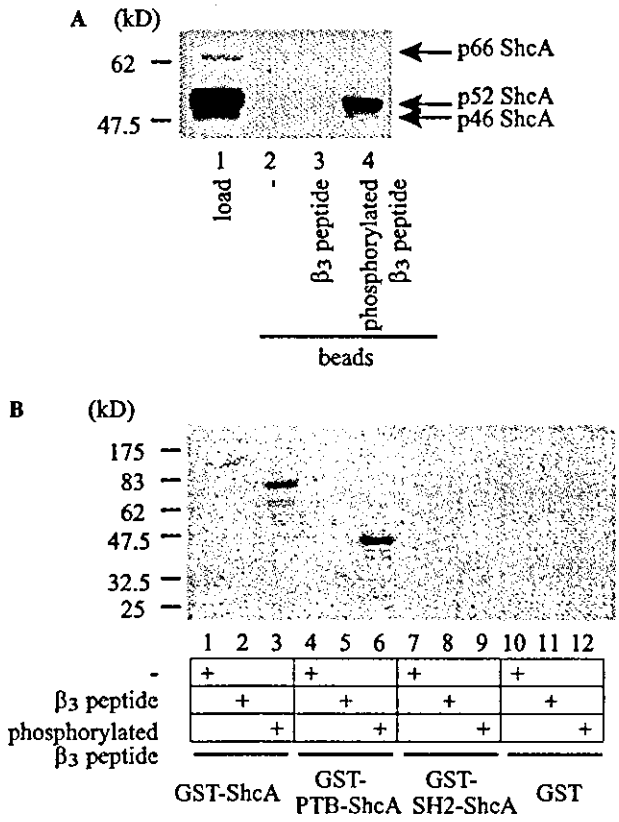

Fig. 2. ShcA binds to tyrosine-phosphorylated β_3 peptide through its PTB domain. (A) Streptoavidin beads alone (lane 2), and the beads coated with the tyrosine-phosphorylated (lane 4) and non-phosphorylated β_3 peptide (lane 3) were incubated with platelet cytosol (lane 1), and bead-associated ShcA was analyzed by immunoblot as described in the Experimental procedures. The data shown are the representative of three independent experiments with similar results. (B) Biotin-coated streptoavidin beads (lanes 1, 4, 7, and 10), and beads coated with the biotin-tyrosine-phosphorylated (lanes 3, 6, 9, and 12) and biotin-non-phosphorylated β_3 peptides (lanes 2, 5, 8, and 11) were incubated with 100 pmol GST-ShcA (lanes 1–3), GST-PTB-ShcA (lanes 4–6), GST-SH2-ShcA (lanes 7–9), and GST (lanes 10–12) and the bead-associated proteins were analyzed by immunoblot with anti-GST antibody as described in the Experimental Procedures. The data shown are the representative of three independent experiments with similar results.

domain, mediates the direct binding to the tyrosine-phosphorylated β_3 peptide. We generated and purified proteins of GST-ShcA, GST-PTB-ShcA, GST-SH2-ShcA, and GST in *E. coli*. Then, we incubated these proteins with streptoavidin-beads coated with β_3-tail peptides. As shown in Fig. 2B, PTB-ShcA bound to the phosphorylated β_3 peptide (lane 6), but not to the non-phosphorylated peptide (lane 5) or biotin (lane 4). On the other hand, SH2-ShcA did not bind to either of β_3 peptides (lanes 7–9). Thus, ShcA bound to the tyrosine-phosphorylated, but not non-phosphorylated, β_3 peptide through its PTB domain.

So far, myosin [6] and the adaptor protein ShcA [7] have been shown to bind to the tyrosine-phosphorylated β_3-tail. While binding of myosin requires phosphorylation of both tyrosine residues, ShcA-binding requires only Y759 phosphorylation [7]. The binding of proteins to the phosphotyrosine-containing motifs is known to depend upon the sequences around phosphorylated tyrosine. Although the sequence NITYRGT around Y759 of β_3 does not contain the SH2-domain-binding pYXNX motif, it contains the PTB-domain-binding NXXpY motif [18]. It is conceivable that ShcA interacts with the NITpY(759) of β_3 through its PTB domain.

We have previously established an assay for analyzing the Ca^{2+}-induced aggregation of platelets permeabilized with streptolysin-O using a light transmission aggregometer [12]. The aggregation of permeabilized platelets in the assay revealed similar responses in Ca^{2+}-sensitivity, time course, and involvement of the integrin to that of intact platelets [12]. Reconstitution of aggregation of permeabilized platelets in the assay required exogenous addition of platelet cytosol [12]. Since most of p52 ShcA was present in the cytosol of platelets (Fig. 1B), to examine whether ShcA is involved in the regulation of aggregation, we specifically depleted the platelet cytosol of ShcA with anti-ShcA antibody-coated beads (Fig. 3A). While the platelet cytosol treated with the control rabbit IgG-coated beads retained the supporting activity for the Ca^{2+}-induced platelet aggregation in the assay, the ShcA-depleted cytosol lost the aggregation-supporting activity (Fig. 3C). We produced GST-p52 ShcA with baculovirus-expression system and purified the protein from overexpressing Sf9 cells (Fig. 3B). As shown in Fig. 3C, addition of purified GST-ShcA concentration-dependently rescued the aggregation-supporting activity of the ShcA-depleted cytosol. Thus, ShcA is an essential factor in platelet cytosol for the Ca^{2+}-induced platelet aggregation.

By using this semi-intact aggregation assay, we previously demonstrated that PKCα is an essential cytosolic factor for platelet aggregation by showing that the PKC-depleted cytosol lost the aggregation-supporting activity that was rescued by addition of purified PKCα [12]. In that study, addition of PKCα alone without addition of any cytosol did not support the aggregation [12]. Therefore, we speculated that cytosolic factor(s) other than PKCα are also required for the aggregation [12]. With the results presented here, we could say that one of such factors is ShcA. It has been demonstrated that phosphorylation of ShcA by PKCα promotes its membrane translocation [19,20]. ShcA and PKCα might cooperatively regulate platelet aggregation.

Talin, an actin binding protein, has been demonstrated to bind to β_3-tail and regulate activity of the integrin $\alpha_{IIb}\beta_3$ [5,21,22]. CIB (calcium and integrin binding protein) [23,24] and β-endonexin [25] bind to α_{IIb}-tail and regulate this integrin activity. Here, we showed the involvement of ShcA in this regulation. Thus, the

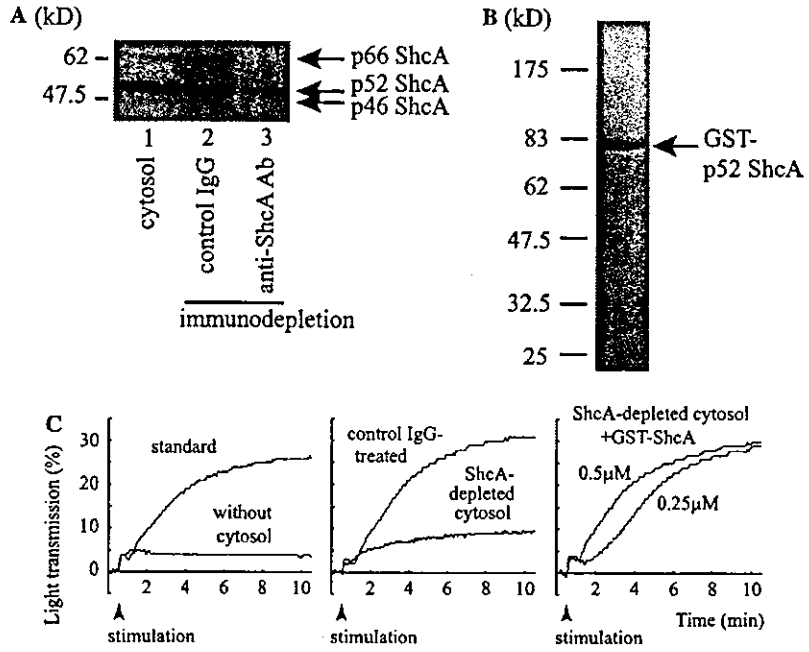

Fig. 3. ShcA-depleted cytosol loses the aggregation-supporting activity, which is rescued by addition of purified recombinant ShcA. (A) Platelet cytosol (lane 1) was incubated with anti-ShcA antibody (lane 3) or control IgG (lane 2)-coated beads, and, after removing these beads, the supernatants were analyzed by immunoblot with anti-ShcA antibody as described in Experimental procedures. (B) GST-p52 ShcA purified from Sf9 cells was analyzed in Coomassie-stained SDS–PAGE gel. (C) The Ca^{2+}-induced aggregation of the permeabilized platelets was examined in the presence of platelet cytosol, cytosol treated with the control IgG, and the ShcA-depleted cytosol in the absence or presence of 0.25 and 0.5 μM GST-ShcA purified from Sf9 cells as described in Experimental procedures. The data shown are the representative of three independent experiments with similar results.

activity of the integrin is regulated by multiple factors at its cytosolic tail. It is essential to elucidate the mechanism of how these factors cooperatively or independently regulate the integrin activation for further understanding of platelet aggregation.

In summary, we have directly demonstrated that the adaptor protein ShcA regulates the platelet aggregation most likely through direct interaction with tyrosine-phosphorylated β_3 subunit. Further investigation of the mechanism of ShcA-mediated platelet aggregation would provide a clue for understanding of the process of platelet aggregation.

Acknowledgments

We are also grateful to the Kyoto Red Cross Blood Center for providing platelet pellet and to T. Matsubara for excellent technical assistance. This work was supported by Research Grants from Ministry of Education, Culture, Sports, Science and Technology, Japan (No. 16-1244 to R.S., 12CE2006 and 16209031 to T.K., and No. 15590740 and 15081206 to H.H.,), Health and Labour Sciences Research Grants from Research Grants from Ministry of Health Labour and Welfare, Japan (Comprehensive Research on Aging and Health (H14-Tyouju-012) to T.K. and H.H.), and partially by grants from Takeda Science Foundation, Suzuken Memorial Foundation, Study Group of Molecular Cardiology and Novartis Foundation for Gerontological Research to H.H.

References

[1] R.O. Hynes, Integrins: bidirectional, allosteric signaling machines, Cell 110 (2002) 673–687.
[2] O. Vinogradova, A. Velyvis, A. Velyviene, B. Hu, T. Haas, E. Plow, J. Qin, A structural mechanism of integrin alpha(IIb)beta(3) "inside-out" activation as regulated by its cytoplasmic face, Cell 110 (2002) 587–597.
[3] D.R. Phillips, K.S. Prasad, J. Manganello, M. Bao, L. Nannizzi-Alaimo, Integrin tyrosine phosphorylation in platelet signaling, Curr. Opin. Cell Biol. 13 (2001) 546–554.
[4] D.A. Law, L. Nannizzi-Alaimo, D.R. Phillips, Outside-in integrin signal transduction. Alpha IIb beta 3-(GP IIb IIIa) tyrosine phosphorylation induced by platelet aggregation, J. Biol. Chem. 271 (1996) 10811–10815.
[5] D.A. Law, F.R. DeGuzman, P. Heiser, K. Ministri-Madrid, N. Killeen, D.R. Phillips, Integrin cytoplasmic tyrosine motif is required for outside-in alphaIIbbeta3 signalling and platelet function, Nature 401 (1999) 808–811.
[6] A.L. Jenkins, L. Nannizzi-Alaimo, D. Silver, J.R. Sellers, M.H. Ginsberg, D.A. Law, D.R. Phillips, Tyrosine phosphorylation of the beta3 cytoplasmic domain mediates integrin-cytoskeletal interactions, J. Biol. Chem. 273 (1998) 13878–13885.
[7] K.J. Cowan, D.A. Law, D.R. Phillips, Identification of shc as the primary protein binding to the tyrosine-phosphorylated beta 3 subunit of alpha IIbbeta 3 during outside-in integrin platelet signaling, J. Biol. Chem. 275 (2000) 36423–36429.

[8] G. Pelicci, L. Dente, A. De Giuseppe, B. Verducci-Galletti, S. Giuli, S. Mele, C. Vetriani, M. Giorgio, P.P. Pandolfi, G. Cesareni, P.G. Pelicci, A family of Shc related proteins with conserved PTB, CH1 and SH2 regions, Oncogene 13 (1996) 633–641.

[9] K.S. Ravichandran, Signaling via Shc family adapter proteins, Oncogene 20 (2001) 6322–6330.

[10] K.M. Lai, T. Pawson, The ShcA phosphotyrosine docking protein sensitizes cardiovascular signaling in the mouse embryo, Genes Dev. 14 (2000) 1132–1145.

[11] L. Bonfini, E. Migliaccio, G. Pelicci, L. Lanfrancone, P.G. Pelicci, Not all Shc's roads lead to Ras, Trends Biochem. Sci. 21 (1996) 257–261.

[12] A. Tabuchi, A. Yoshioka, T. Higashi, R. Shirakawa, H. Nishioka, T. Kita, H. Horiuchi, Direct demonstration of involvement of protein kinase Calpha in the Ca2+-induced platelet aggregation, J. Biol. Chem. 278 (2003) 26374–26379.

[13] M. Palmer, R. Harris, C. Freytag, M. Kehoe, J. Tranum-Jensen, S. Bhakdi, Assembly mechanism of the oligomeric streptolysin O pore: the early membrane lesion is lined by a free edge of the lipid membrane and is extended gradually during oligomerization, EMBO J. 17 (1998) 1598–1605.

[14] A. Fabiato, F. Fabiato, Calculator programs for computing the composition of the solutions containing multiple metals and ligands used for experiments in skinned muscle cells, J. Physiol. (Paris) 75 (1979) 463–505.

[15] U.K. Laemmli, Cleavage of structural proteins during the assembly of the head of bacteriophage T4, Nature 227 (1970) 680–685.

[16] G. Pelicci, L. Lanfrancone, F. Grignani, J. McGlade, F. Cavallo, G. Forni, I. Nicoletti, T. Pawson, P.G. Pelicci, A novel transforming protein (SHC) with an SH2 domain is implicated in mitogenic signal transduction, Cell 70 (1992) 93–104.

[17] E. Migliaccio, S. Mele, A.E. Salcini, G. Pelicci, K.M. Lai, G. Superti-Furga, T. Pawson, P.P. Di Fiore, L. Lanfrancone, P.G. Pelicci, Opposite effects of the p52shc/p46shc and p66shc splicing isoforms on the EGF receptor-MAP kinase-fos signalling pathway, EMBO J. 16 (1997) 706–716.

[18] W.M. Kavanaugh, L.T. Williams, An alternative to SH2 domains for binding tyrosine-phosphorylated proteins, Science 266 (1994) 1862–1865.

[19] L. Daulhac, A. Kowalski-Chauvel, L. Pradayrol, N. Vaysse, C. Seva, Ca2+ and protein kinase C-dependent mechanisms involved in gastrin-induced Shc/Grb2 complex formation and P44-mitogen-activated protein kinase activation, Biochem. J. 325 (Part 2) (1997) 383–389.

[20] C.K. Miranti, S. Ohno, J.S. Brugge, Protein kinase C regulates integrin-induced activation of the extracellular regulated kinase pathway upstream of Shc, J. Biol. Chem. 274 (1999) 10571–10581.

[21] D.A. Calderwood, B. Yan, J.M. de Pereda, B.G. Alvarez, Y. Fujioka, R.C. Liddington, M.H. Ginsberg, The phosphotyrosine binding-like domain of talin activates integrins, J. Biol. Chem. 277 (2002) 21749–21758.

[22] S. Tadokoro, S.J. Shattil, K. Eto, V. Tai, R.C. Liddington, J.M. de Pereda, M.H. Ginsberg, D.A. Calderwood, Talin binding to integrin beta tails: a final common step in integrin activation, Science 302 (2003) 103–106.

[23] U.P. Naik, P.M. Patel, L.V. Parise, Identification of a novel calcium-binding protein that interacts with the integrin alphaIIb cytoplasmic domain, J. Biol. Chem. 272 (1997) 4651–4654.

[24] S. Tsuboi, Calcium integrin-binding protein activates platelet integrin alpha IIbbeta 3, J. Biol. Chem. 277 (2002) 1919–1923.

[25] H. Kashiwagi, M.A. Schwartz, M. Eigenthaler, K.A. Davis, M.H. Ginsberg, S.J. Shattil, Affinity modulation of platelet integrin alphaIIbbeta3 by beta3-endonexin, a selective binding partner of the beta3 integrin cytoplasmic tail, J. Cell Biol. 137 (1997) 1433–1443.

Geriatrics and Gerontology International 2004; 4: 151–156

ORIGINAL ARTICLE

Strategy for treating elderly Japanese with hypercholesterolemia*

Hisanori Horiuchi,[1] Yuji Matsuzawa,[2] Hiroshi Mabuchi,[3] Hiroshige Itakura,[4] Jun Sasaki,[5] Mitsuhiro Yokoyama,[6] Yuichi Ishikawa,[7] Shinji Yokoyama,[8] Seijiro Mori,[9] Takashi Ohrui,[10] Masahiro Akishita,[11] Toshio Hayashi,[12] Kiminori Yamane,[13] Genshi Egusa[14] and Toru Kita[15]

[1]Departments of Geriatric Medicine and [15]Cardiovascular Medicine, Graduate School of Medicine, Kyoto University, Kyoto, [2]Department of Internal Medicine, The Sumitomo Hospital, Osaka, [3]The Second Department of Internal Medicine, School of Medicine, Kanazawa University, Kanazawa, [4]Ibaraki Christian University, Ibaraki, [5]International University Graduate School of Health and Welfare, Fukuoka, [6]Division of Cardiovascular and Respiratory Medicine, Department of Internal Medicine, Kobe University Graduate School of Medicine and [7]Faculty of Health Sciences, Kobe University School of Medicine, Kobe, [8]Department of Biochemistry, Cell Biology and Metabolism, Nagoya City University Graduate School of Medical Sciences, and [12]Department of Geriatrics, Nagoya University Graduate School of Medicine, Nagoya, [9]Department of Internal Medicine, Matsudo Municipal Hospital, Matsudo, [10]Department of Geriatric and Respiratory Medicine, Tohoku University School of Medicine, [11]Department of Geriatric Medicine, Kyorin University School of Medicine, Mitaka, [13]The Second Department of Internal Medicine, Hiroshima University School of Medicine, and [14]The Egusa Genshi Clinic, Hiroshima, Japan

Background: It has been widely accepted that control of serum cholesterol levels is effective for prevention of cardiovascular events. Recent data have suggested that this is also the case in the elderly.

Methods: A research group (chaired by T. Kita) was organized as part of the Comprehensive Research on Aging and Health conducted by the Japanese Ministry for Health, Labour, and Welfare in 1999–2002 to determine the best strategy for control of cholesterol levels in elderly Japanese with hypercholesterolemia. In order to do this a review of the literature was conducted.

Conclusion: The research group concluded: (i) Japanese patients aged 65–74 years with hypercholesterolemia should be treated by following the Guideline for Diagnosis and Treatment of Atherosclerotic Cardiovascular Diseases by the Japan Atherosclerosis Society (2002), as cholesterol-lowering therapy would bring a similar, or even larger, preventive effect to the elderly, whose absolute risk of cardiovascular events is higher than that in the younger population; (ii) target cholesterol levels in elderly Japanese aged ≥ 75 years with

Accepted for publication 17 February 2004.

Correspondence: Dr Toru Kita, Department of Cardiovascular Medicine, Graduate School of Medicine, Kyoto University, Kyoto, 606–8507, Japan. Email: tkita@kuhp.kyoto-u.ac.jp

*Based on the report of the Research Group for 'Long-term prognosis of elderly Japanese with hypercholesterolemia' in the Comprehensive Research on Aging and Health.

hypercholesterolemia should be determined individually according to their physical activities. It is noted that the elderly are more susceptible to drug-related adverse effects than the younger since renal and liver functions, required for metabolizing drugs, in the elderly are relatively weaker.

Keywords: cardiovascular event, elderly, hypercholesterolemia, Japanese, statin.

Introduction

It is well known that cardiovascular events occur in elderly people more frequently than in the younger population. It is also known that the incidence of these events increases as serum cholesterol levels are elevated. In Japan, populations of elderly people are rapidly increasing and serum cholesterol levels have been clearly rising in all ranges of ages probably due to westernization of our dietary habits.[1] Therefore, a rapid increase in atherosclerotic diseases is anticipated in Japan, especially in the elderly, without appropriate prevention.

Data obtained in many clinical studies performed in Western countries have demonstrated that cholesterol-lowering therapy with HMG-CoA reductase inhibitors, statins, reduces cardiovascular events by 26–37%.[2–4] Therefore, therapeutic intervention to control serum cholesterol levels is widely accepted. So far, guidelines for controlling cholesterol levels have been established in several countries, such as ATPIII (http://www.nhlbi.nih.gov/guidelines/cholesterol/atp_iii.htm) in the USA. Since the incidence of cardiovascular events in the Japanese population is clearly lower than that in Western countries, establishment of the Japanese guideline has been considered necessary. The first Japanese guideline was established by the Japanese Atherosclerosis Society in 1997 and it has been revised in 2002 (http://jas.umin.ac.jp). Since the subjects for the guideline are those aged ≤ 65 years, the guideline for elderly Japanese has been expected to be established.

In 1996–99, the research group for 'Establishing Japanese guidelines for treating atherosclerotic diseases in the elderly' was organized as part of the Comprehensive Research on Aging and Health conducted by the Japanese Ministry for Health, Labour and Welfare and the first guideline was proposed in 1999 (Kita & Hata *et al.* unpublished report to the Japanese Ministry of Health and Welfare 1999). In this guideline, the target cholesterol levels for the elderly were recommended to be 20 mg/dL higher than those for the younger population, based on the comparison of relative risk increase in relation to serum cholesterol levels between younger people and the elderly (Kita & Hata *et al.* unpublished report to the Japanese Ministry of Health and Welfare 1999). Since then, several important clinical datasets in Western countries and results of studies conducted in Japan,[2–4] such as the KLIS,[5,6] the J-LIT and PATE have been produced.[7–9] Therefore, the research group was again organized in 1999–2002 in order to conduct a research project entitled 'Long-term prognosis of the elderly with hyperlipidemia' (chaired by T. Kita) as a part of the Comprehensive Research on Aging and Health with a view to re-evaluating the proposed guideline (Kita & Hata *et al.* unpublished report to the Japanese Ministry of Health and Welfare 1999). The research group has concluded that serum cholesterol levels in Japanese aged 65–74 years are recommended to be controlled in the same way as for patients aged ≤ 65 years by following the Guideline for Diagnosis and Treatment of Atherosclerotic Cardiovascular Diseases (2002) by the Japan Atherosclerosis Society (http://jas.umin.ac.jp/), and that for those aged ≥ 75 years the control levels should be determined individually based on their physical activities (Kita & Matsuzawa *et al.* unpublished report to the Japanese Ministry of Health and Welfare 2002).

Clinical data in Western countries

Secondary prevention studies such as 4S and CARE have been analyzed with a focus on the elderly.[10,11] In both studies, treatment with simvastatin and pravastatin in the elderly patients was as safe and effective for reducing serum cholesterol levels as it was in younger patients.[10,11] In the 4S study, 4444 patients with established coronary heart diseases were divided into simvastatin and placebo groups, and followed for 5.4 years.[10] In this study, simvastatin treatment reduced total cholesterol levels by 26% in the elderly aged 65–70 years and by 25% in younger patients,[10] indicating that the cholesterol lowering effect of simvastatin in the elderly is similar to that in the younger. The relative risk reduction of major coronary events, including coronary artery death and non-fatal myocardial infarction, by simvastatin in the elderly patients was 34%, similar to that in younger patients aged < 65 years.[10] In the CARE study, 4159 patients were divided into pravastatin and placebo groups and followed for 5 years.[11] In this study, pravastatin treatment reduced total cholesterol levels by 19% in the elderly aged 65–75 years and by 20% in patients aged < 65 years,[11] indicating that the cholesterol lowering effect of simvastatin in the elderly is similar to that in younger patients. The relative risk reduction in the elderly group was 39% while that in the younger was 13%.[11] Because of the higher absolute risk and greater effect on risk reduction in the elderly group, the number

needed to treat (NNT) in the 5-year follow-up period in the elderly group was 15 while that in the younger group was 67.[11]

Recently, the results of the PROSPER study have been published.[12] In this study, approximately 5800 high-risk patients aged 70–82 (mean 75 years) with normal total cholesterol levels (mean 217 mg/dL) were divided into pravastatin and placebo groups, and followed for 3 years. In this elderly population, the statin reduced coronary events by 19%. Since the preventive effects by statins become obvious in 1–2 years after starting the medication in many studies,[2-4] the risk reduction ratio in the PROSPER study could be relatively smaller during the 3-year follow-up period.[12] In the ASCOT study, approximately 19 000 hypertensive high-risk patients with total cholesterol levels of ≤ 250 mg/dL (213 mg/dL average), aged 40–79 years (mean 63 years), were assigned into placebo and 10 mg/day atorvastatin groups, and followed for 3 years.[13] The results showed that treatment with atorvastatin reduced coronary events by 36%. The risk reduction in the subgroup aged ≥ 60 years was also 36%, which was similar to that in younger patients aged < 60 years. Thus, it has been demonstrated in studies conducted in Western countries that cholesterol-lowering therapy in the elderly brings similar, or even better, effects in the prevention of coronary events, compared with its effects on younger patients.

It has been demonstrated that cholesterol lowering therapy by statins slowed the narrowing of coronary arteries and reduced intima-media thickness in carotid arteries.[14,15] Thus, cholesterol lowering by statins could stabilize atheromatous plaque, thereby inhibiting the event occurrence.

Clinical data in Japan

The Hisayama study was an epidemiological study conducted in the Hisayama community in Japan.[16] In this study, where 2673 people aged ≥ 40 years were followed from 1988 to 1996, the absolute risk for ischemic heart diseases (myocardial infarction and sudden death) was reported to be 2.3/1000/year and that for cerebral infarction to be 3.1/1000/year.[17]

The J-LIT study was a cohort observational study in Japan. In this study, approximately 50 000 hypercholesterolemic patients aged ≤ 70 years undergoing 5–10 mg/day simvastatin treatment were followed for 6 years. A subanalysis focusing on elderly patients without prior coronary events was performed.[18] In both the elderly group, aged 65–70 years (mean 67 years) and consisting of 9860 patients, and the younger group, aged ≤ 64 years (mean 55 years) and consisting of 32 500 patients, total cholesterol levels were approximately 270 mg/dL at enrollment and 210–220 mg/dL during follow-up periods under simvastatin treatment. Changes in low-density lipoprotein (LDL)-cholesterol levels were also similar: levels of approximately 180 mg/dL at the baseline were reduced to approximately 130 mg/dL in the follow-up periods in both groups. No severe drug-related adverse effects occurred in either group. Thus, statin treatment in the elderly is as safe and effective for reducing serum cholesterol levels as it is in younger patients. The doses of the statin were lower than those used in Western countries, where 20–40 mg/day simvastatin was used.[2]

In the J-LIT study, the incidence of coronary events (sudden cardiac death and acute myocardial infarction) in the elderly was 1.30/1000/year and that in the younger 0.8/1000/year. When occurrence of angina was included in coronary events, the incidence in the elderly was 2.25/1000/year and that in the younger 1.35/1000/year. Cox-biohazard analysis revealed that the relative risks of coronary events increased by 1.7% as serum LDL-cholesterol levels increased by 1 mg/dL, which were similar in both groups.[18] Importantly, in any LDL-cholesterol levels, the absolute risk in the elderly was higher than that in the younger. Generally, coronary events occur twice as often in men as in women, which was also observed in the J-LIT study.[7,8] In the J-LIT study, 35% of the study subjects were male in the younger group and 21% were male in the elderly group.[18] Therefore, upon interpretation of this J-LIT data, the male : female ratio should be considered. Indeed, in male patients, the coronary events (sudden cardiac death and acute myocardial infarction) occurred at a rate of 2.45/1000 patients/year in the elderly and 1.41/1000 patients/year in younger patients.

The KLIS study was planned as a primary prevention study for male patients aged 45–74 years with serum cholesterol levels ≥ 220 mg/dL.[5,6] Enrolled patients were assigned into a conventional therapy group and a pravastatin group, and followed for 5 years. However, since the results of several studies revealed superior effects of statin therapy for the event prevention during the study period, the assignment could not be kept completely. As a result, 2219 cases in the pravastatin group and 1634 cases in the conventional therapy group were analyzed. Coronary events (sudden death, myocardial infarction, coronary intervention and bypass surgery) occurred in 5.95/1000 per year in the conventional therapy group and 5.77/1000 per year in the pravastatin group. Cerebral infarction occurred in 5.15/1000 per year in the conventional therapy group and 4.19/1000 per year in the pravastatin group. In the pravastatin group, 1105 cases were of good compliance for the drug-intake. The relative risk of coronary events plus cerebral infarction of the good-compliance group was 0.57 (0.54–0.98) compared with that of the conventional therapy group. A subanalysis examining those aged ≥ 65 years in this study revealed a tendency similar to that observed in the J-LIT study.[18] Namely, coronary events increased as

serum LDL-cholesterol levels increased in both elderly and younger groups, and the absolute risks in the elderly were higher than those in the younger in any given LDL-levels (Sasaki *et al.* in preparation).

In the PATE study, 665 patients (male ratio 21%) aged ≥ 60 years (mean 73 years) with serum total cholesterol levels of 220–280 mg/dL were followed for 3–5 years (mean 3.9 years) under treatment with low-dose (5 mg) or high-dose (10–20 mg) pravastatin.[9] In this study, events were defined as cerebral bleeding, cerebral infarction, transient ischemic attack, subarachnoid hemorrhage, myocardial infarction, angina pectoris, cardiac failure, arrhythmia, arteriosclerosis obliterance, dissecting aortic aneurysm, and peripheral artery thrombosis. During the follow-up period, acute myocardial infarction occurred in 11 cases (4.2/1000/year). In the patient group without diabetes and with serum cholesterol levels of < 253 mg/dL and triglyceride levels of ≥ 133 mg/dL, the event-free ratio in the high-dose group was significantly higher than that in the low-dose group.

Thus, we could expect similar, or even more beneficial, effects of cholesterol-lowering therapy to reduce cardiovascular events in elderly Japanese compared with those in the younger population, although the studies described above appear to be somewhat indirect. Urgently and absolutely required are complete epidemiological and/or interventional large-scale studies, from which we can definitely estimate the absolute risks and the risk reduction rates in the current Japanese population.

Cerebral infarction and hypercholesterolemia

Cerebral infarction is also a disease that occurs more frequently in the elderly. Cerebral infarction is classified into following three: (i) lacunar infarction caused by small artery occlusion which is correlated with hypertension; (ii) cardiogenic cerebral embolism, which is usually associated with atrial fibrillation; and (iii) cerebral infarction caused by atherothrombotic arterial occlusion. Hypercholesterolemia is considered to be linked to atherothrombotic occlusion.

In the 4S secondary prevention study, simvastatin reduced total strokes by 35%.[2] The data obtained in secondary prevention studies with pravastatin, including the LIPID and CARE studies, have been combined and analyzed.[19] The results demonstrated that pravastatin treatment reduced total strokes by 22% and non-hemorrhagic strokes by 23%.[19] In the ASCOT study, atorvastatin reduced fatal and non-fatal strokes by 27%.[13] In the MRC/BHF Heart Protection Study, where approximately 20 000 high-risk patients aged 40–80 years had been randomly assigned into placebo and simvastatin-treated groups and followed for 5 years, simvastatin reduced ischemic strokes by 29%.[20] In the KLIS study conducted in Japan, the incidence of cerebral infarction was 5.15/1000 per year in the conventional therapy group and 4.19/1000 per year in the pravastatin group.[5,6] In the KLIS study, the incidence of cerebral infarction increased as LDL-cholesterol levels increased in elderly aged ≥ 65 years (Sasaki *et al.* in preparation). In the J-LIT study, the incidence of ischemic cerebrovascular events was 1.41/1000 per year in the subgroup without prior coronary or cerebral infarction (Nakaya *et al.* unpublished data). In both studies, the incidence of ischemic cerebral events was clearly higher in the elderly than that in the younger. Thus, evidence is accumulating to support the preventive effects of serum cholesterol-lowering on the occurrence of cerebral infarction. We may expect risk reduction for not only coronary events but also cerebral infarction in cholesterol-lowering therapy. Although the incidence of coronary events in Japan is much lower compared with that in Western countries, the incidence of cerebrovascular events are similar. Since incidence of cerebrovascular events in Japan is similar to that of coronary events, impact of the prevention of cerebrovascular events is as large as that of coronary events in Japan.

Conclusions: Strategy for treating elderly Japanese with hypercholesterolemia

As reviewed above, the control of serum cholesterol levels appears effective in risk reduction of cardiovascular events in elderly Japanese as well as in the younger population. The incidence of such events in the elderly is generally higher than that in younger people. Therefore, the elderly would be even more suitable subjects for preventative intervention. Although it may take long periods to develop atherosclerosis, the preventive effects for cardiovascular events become apparent in 1–2 years after cholesterol-lowering therapy has started, as demonstrated in many studies.[2,3,11,12,20] Therefore, it is not too late for us to start cholesterol-lowering therapy in the elderly. We have concluded after discussion in the research group 'Long-term prognosis of elderly Japanese with hypercholesterolemia' that we could expand the subjects of the Guideline for Diagnosis and Treatment of Atherosclerotic Cardiovascular Diseases by the Japan Atherosclerosis Society (2002) to include elderly Japanese aged ≤ 74 years (Kita & Matsuzawa *et al.* unpublished report to the Japanese Ministry of Health and Welfare 2002). In the guideline, patients are divided into several categories based on risk factors and the target cholesterol levels for each category is indicated (http://jas.umin.ac.jp/). Aging, ≥ 45 years for men and ≥ 55 years for women, is defined as a risk factor. Therefore, the target total cholesterol level for the elderly aged 65–74 years without additional risk factors is to be less

than 220 mg/dL and the target LDL-cholesterol level, less than 140 mg/dL. The target levels become lower when elderly patients possess additional risk factors. As described in the guideline (http://jas.umin.ac.jp/), the control of cholesterol levels should be started by changing life styles, followed by drug therapy when appropriate cholesterol levels are not obtained.

For the elderly aged ≥ 75 years, few data for Japanese are available at the moment. Furthermore, it was reported that all causes of mortality increased in the group with lower total cholesterol levels due to an increase in death from infections and malignant tumors in an investigation in Holland, where people aged ≥ 85 years were enrolled.[21] Furthermore, in the Honolulu Heart Program, Japanese–Americans aged 75–93 years (mean 78 years) with a mean total cholesterol level of 149 mg/dL have been reported to have higher mortality than the other groups with the levels at 178, 199 and 232 mg/dL.[22] The physical and nutritional conditions of the highly-aged elderly are various and low cholesterol levels may reflect their worsened health conditions. Therefore, we concluded that, for the highly-aged elderly ≥ 75 years, the target cholesterol levels should be determined individually according to physical and nutritional factors, although a higher absolute risk of cardiovascular events would be expected in the elderly aged ≥ 75 years.

Finally, we again emphasize that physicians should be more careful in their use of drugs in elderly patients since physiological functions of the elderly, such as renal and liver functions required for metabolizing drugs, are not as good as those of the younger patients.

The recommended strategy for treatment for elderly Japanese with hypercholesterolemia

Patients aged 65–74 years

Follow the Guideline for Diagnosis and Treatment of Atherosclerotic Cardiovascular Diseases by the Japan Atherosclerosis Society (2002) (http://jas.umin.ac.jp/).

Patients aged ≥ 75 years

The target values of total and LDL-cholesterol levels should be determined individually.

Points of consideration for treatment of elderly with hypercholesterolemia

1 Cholesterol-lowering therapy reduces relative risk of coronary events in not only the younger but also in the elderly to a similar extent.
2 The elderly would be even more suitable subjects of lipid-lowering therapy, since the absolute risk in the elderly is higher than that in the younger.
3 The elderly might be more susceptive to drug-related adverse effects than the younger since renal and liver functions, required for metabolizing drugs, in the elderly are weaker.

Acknowledgment

The research was supported by a research grant (H11-tyouju-017) for 'Long-term prognosis of elderly Japanese with hypercholesterolemia' in the Comprehensive Research on Aging and Health conducted by the Japanese Ministry for Health, Labour and Welfare, Japan.

References

1 Kuzuya M, Ando F, Iguchi A, Shimokata H. Changes in serum lipid levels during a 10-year period in a large Japanese population. A cross-sectional and longitudinal study. *Atherosclerosis* 2002; **163**: 313–320.
2 The Scandinavian Simvastatin Survival Study Group. Randomised trial of cholesterol lowering in 4444 patients with coronary heart disease: the Scandinavian Simvastatin Survival Study (4S). *Lancet* 1994; **344**: 1383–1389.
3 Shepherd J, Cobbe SM, Ford I *et al.* Prevention of coronary heart disease with pravastatin in men with hypercholesterolemia. West of Scotland Coronary Prevention Study Group. *N Engl J Med* 1995; **333**: 1301–1307.
4 Sacks FM, Tonkin AM, Shepherd J *et al.* Effect of pravastatin on coronary disease events in subgroups defined by coronary risk factors: the Prospective Pravastatin Pooling Project. *Circulation* 2000; **102**: 1893–1900.
5 The Kyushu Lipid Intervention Study Group. Pravastatin use and risk of coronary events and cerebral infarction in Japanese men with moderate hypercholesterolemia: the Kyushu Lipid Intervention Study. *J Atheroscler Thromb* 2000; **7**: 110–121.
6 Sasaki J, Arakawa K, Iwashita M, Matsushita Y, Kono S. Reduction in serum total cholesterol and risks of coronary events and cerebral infarction in Japanese men: the Kyushu Lipid Intervention Study. *Circ J* 2003; **67**: 473–478.
7 Matsuzaki M, Kita T, Mabuchi H *et al.* Large scale cohort study of the relationship between serum cholesterol concentration and coronary events with low-dose simvastatin therapy in Japanese patients with hypercholesterolemia. *Circ J* 2002; **66**: 1087–1095.
8 Mabuchi H, Kita T, Matsuzaki M *et al.* Large scale cohort study of the relationship between serum cholesterol concentration and coronary events with low-dose simvastatin therapy in Japanese patients with hypercholesterolemia and coronary heart disease: secondary prevention cohort study of the Japan Lipid Intervention Trial (J-LIT). *Circ J* 2002; **66**: 1096–1100.
9 Ito H, Ouchi Y, Ohashi Y *et al.* A comparison of low versus standard dose pravastatin therapy for the prevention of cardiovascular events in the elderly: the pravastatin antiatherosclerosis trial in the elderly (PATE). *J Atheroscler Thromb* 2001; **8**: 33–44.
10 Miettinen TA, Pyorala K, Olsson AG *et al.* Cholesterol-lowering therapy in women and elderly patients with myocardial infarction or angina pectoris: findings from the Scandinavian Simvastatin Survival Study (4S). *Circulation* 1997; **96**: 4211–4218.
11 Lewis SJ, Moye LA, Sacks FM *et al.* Effect of pravastatin on cardiovascular events in older patients with myocardial

infarction and cholesterol levels in the average range. Results of the Cholesterol and Recurrent Events (CARE) trial. *Ann Intern Med* 1998; **129**: 681–689.
12 Shepherd J, Blauw GJ, Murphy MB *et al.* Pravastatin in elderly individuals at risk of vascular disease (PROSPER): a randomised controlled trial. *Lancet* 2002; **360**: 1623–1630.
13 Sever PS, Dahlof B, Poulter NR *et al.* ASCOT investigators. Prevention of coronary and stroke events with atorvastatin in hypertensive patients who have average or lower than-average cholesterol concentrations, in the Anglo-Scandinavian Cardiac Outcomes Trial-Lipid Lowering Arm (ASCOT-LLA): a multicentre randomised controlled trial. *Lancet* 2002; **361**: 1149–1158.
14 Teo KK, Burton JR, Buller CE *et al.* Long-term effects of cholesterol lowering and angiotensin-converting enzyme inhibition on coronary atherosclerosis: The Simvastatin/ Enalapril Coronary Atherosclerosis Trial (SCAT). *Circulation* 2000; **102**: 1748–1754.
15 Smilde TJ, van Wissen S, Wollersheim H, Trip MD, Kastelein JJ, Stalenhoef AF. Effect of aggressive versus conventional lipid lowering on atherosclerosis progression in familial hypercholesterolaemia (ASAP): a prospective, randomised, double-blind trial. *Lancet* 2001; **357**: 577–581.
16 Tanizaki Y, Kiyohara Y, Kato I *et al.* Incidence and risk factors for subtypes of cerebral infarction in a general population: the Hisayama study. *Stroke* 2000; **31**: 2616–2622.
17 Fujishima M. [Cardiovascular disease in the elderly: the Hisayama Study.] *Nippon Ronen Igakkai Zasshi* 1999; **36**: 16–21. (In Japanese.)
18 Horiuchi H, Kita T, Mabuchi H *et al.* Primary cardiovascular events and serum lipid levels in elderly Japanese with hyperchlesterolemia under 6-year simvastatin treatment: A sub analysis of the J-LIT study. *J Am Geriat Soc* 2004 (in press).
19 Byington RP, Davis BR, Plehn JF *et al.* Reduction of stroke events with pravastatin: the Prospective Pravastatin Pooling (PPP) Project. *Circulation* 2001; **103**: 387–392.
20 Heart Protection Study Collaborative Group. MRC/BHF Heart Protection Study of cholesterol lowering with simvastatin in 20,536 high-risk individuals: a randomised placebo-controlled trial. *Lancet* 2002; **360**: 7–22.
21 Weverling-Rijnsburger AW, Blauw GJ, Lagaay AM, Knook DL, Meinders AE, Westendorp RG. Total cholesterol and risk of mortality in the oldest old. *Lancet* 1997; **350**: 1119–1123.
22 Schatz IJ, Masaki K, Yano K, Chen R, Rodriguez BL, Curb JD. Cholesterol and all-cause mortality in elderly people from the Honolulu Heart Program: a cohort study. *Lancet* 2001; **358**: 351–355.

Roles of thromboxane A_2 and prostacyclin in the development of atherosclerosis in apoE-deficient mice

Takuya Kobayashi,[1] Yoshio Tahara,[1] Mayumi Matsumoto,[1] Masako Iguchi,[1] Hideto Sano,[2] Toshinori Murayama,[3] Hidenori Arai,[2] Hiroji Oida,[4] Takami Yurugi-Kobayashi,[5] Jun K. Yamashita,[5] Hiroyuki Katagiri,[6,7] Masataka Majima,[7] Masayuki Yokode,[3] Toru Kita,[8] and Shuh Narumiya[1]

[1]Department of Pharmacology, [2]Department of Geriatric Medicine, and [3]Department of Clinical Innovative Medicine, Kyoto University Faculty of Medicine, Kyoto, Japan. [4]Fukui Safety Research Institute, Ono Pharmaceutical Co., Fukui, Japan. [5]Laboratory of Stem Cell Differentiation, Kyoto University Faculty of Medicine, Kyoto, Japan. [6]Department of Surgery and [7]Department of Pharmacology, Kitasato University School of Medicine, Kanagawa, Japan. [8]Department of Cardiovascular Medicine, Kyoto University Faculty of Medicine, Kyoto, Japan.

Production of thromboxane (TX) A_2 and PG I_2/prostacyclin (PGI_2) is increased in patients with atherosclerosis. However, their roles in atherogenesis have not been critically defined. To examine this issue, we cross-bred atherosclerosis-prone apoE-deficient mice with mice deficient in either the TXA receptor (TP) or the PGI receptor (IP). Although they showed levels of serum cholesterol and triglyceride similar to those of apoE-deficient mice, *apoE*$^{-/-}$*TP*$^{-/-}$ mice exhibited a significant delay in atherogenesis, and *apoE*$^{-/-}$*IP*$^{-/-}$ mice exhibited a significant acceleration in atherogenesis compared with mice deficient in apoE alone. The plaques in *apoE*$^{-/-}$*IP*$^{-/-}$ mice showed partial endothelial disruption and exhibited enhanced expression of ICAM-1 and decreased expression of platelet endothelial cell adhesion molecule 1 (PECAM-1) in the overlying endothelial cells compared with those of *apoE*$^{-/-}$*TP*$^{-/-}$ mice. Platelet activation with thrombin ex vivo revealed higher and lower sensitivity for surface P-selectin expression in platelets of *apoE*$^{-/-}$*IP*$^{-/-}$ and *apoE*$^{-/-}$*TP*$^{-/-}$ mice, respectively, than in those of *apoE*$^{-/-}$ mice. Intravital microscopy of the common carotid artery revealed a significantly greater number of leukocytes rolling on the vessel walls in *apoE*$^{-/-}$*IP*$^{-/-}$ mice than in either *apoE*$^{-/-}$*TP*$^{-/-}$ or *apoE*$^{-/-}$ mice. We conclude that TXA_2 promotes and PGI_2 prevents the initiation and progression of atherogenesis through control of platelet activation and leukocyte-endothelial cell interaction.

Introduction

It is now understood that atherosclerosis is an inflammation in the intima of large arteries that is triggered by high serum cholesterol and in which various types of cells including monocytes/macrophages, endothelial cells (ECs), smooth muscle cells (SMCs), T cells, and blood platelets exert a complex array of interaction (1). A variety of substances including cytokines, chemokines, and growth factors are suggested to induce, amplify, and modify this inflammatory process. One group of these mediators is prostanoids, which are produced from arachidonic acid by the action of COX and include various types of PGs and thromboxane (TX). Involvement of prostanoids in acute inflammation has been well documented based on the finding that aspirin-like NSAIDs are specific COX inhibitors. Among prostanoids, PG I_2/prostacyclin (PGI_2) and TXA_2 have attracted particular attention for their importance in cardiovascular diseases: the former, generated by vascular ECs, is a potent platelet inhibitor and vasodilator, and the latter, released from activated platelets, is a potent vasoconstrictor and platelet-aggregating agent. Indeed, low-dose aspirin that preferentially inhibits platelet-derived TXA_2 over endothelium-derived PGI_2 has been used as anti-platelet therapy for the prevention of myocardial infarction and recurrence of strokes. Although biosynthesis of PGI_2 and TXA_2 is increased in patients with atherosclerosis (2, 3), the roles of these molecules in the initiation and progression of atherosclerosis have not yet been critically examined.

The role played by prostanoids in atherogenesis has been studied mostly by examining the effects of various drugs in mice deficient in either apoE (*apoE*$^{-/-}$ mice) (4, 5) or the LDL receptor (LDLR) (*LDLR*$^{-/-}$ mice) (6). One group of such pharmacological studies has used low doses of aspirin in atherosclerotic model animals to evaluate the contribution of TXA_2. Cyrus et al. (7) fed *LDLR*$^{-/-}$ mice a high-fat diet, treated the mice with low-dose aspirin, and found that this dose of aspirin significantly retarded the development of atherosclerotic lesions, with a 64% reduction in an en face analysis and 29% in a cross-sectional analysis. In contrast, Cayatte et al. (8) used aspirin in *apoE*$^{-/-}$ mice and did not find retardation in the development of atherosclerotic lesions. This discrepancy could be attributed to the higher dose of aspirin used in the latter study, which may have inhibited prostanoid production in cells other than platelets, particularly PGI_2 in blood vessels. In the same study, Cayatte et al. (8) administered a TXA receptor (TP) antagonist, S-18886, to *apoE*$^{-/-}$ mice. They reported that administration of this drug indeed suppressed the extent of atherogenesis, but only marginally, by 21%. The other group of pharmacological studies has used isoform-specific COX inhibitors and has evaluated the roles of prostanoids in atherogenesis. COX exists as two isoforms encoded by two distinct genes (9): COX-1 is constitu-

Nonstandard abbreviations used: EC, endothelial cell; HDLC, HDL-cholesterol; IP, PGI receptor; LDLC, LDL-cholesterol; LDLR, LDL receptor; PECAM-1, platelet endothelial cell adhesion molecule 1; PFA, paraformaldehyde; PGI_2, PG I_2/prostacyclin; PRP, platelet-rich plasma; SMC, smooth muscle cell; TC, total cholesterol; TG, total triglyceride; TP, TXA receptor; TX, thromboxane; VLDLC, VLDL-cholesterol; vWF, von Willebrand factor.

Conflict of interest: The authors have declared that no conflict of interest exists.

Citation for this article: *J. Clin. Invest.* 114:784-794 (2004). doi:10.1172/JCI200421446.

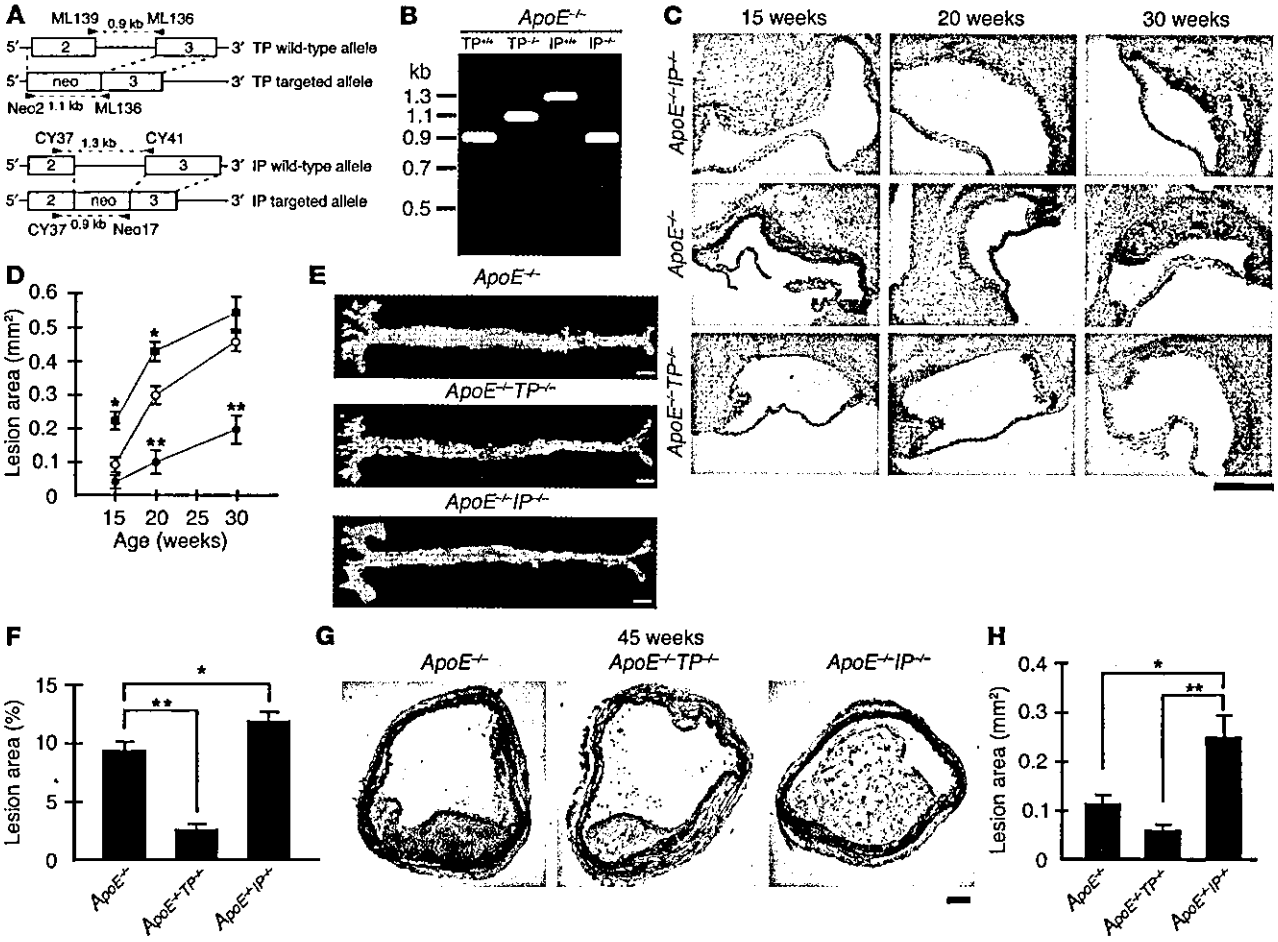

Figure 1

Generation and atherosclerotic lesions of *apoE*$^{-/-}$*TP*$^{-/-}$ and *apoE*$^{-/-}$*IP*$^{-/-}$ mice. (**A**) Strategy for PCR analysis of WT and targeted alleles of TP and IP. Primers are shown by arrowheads. Amplified fragments are shown by broken lines. Neo, neomycin-resistance gene. (**B**) Representative PCR for TP and IP alleles of *apoE*$^{-/-}$, *apoE*$^{-/-}$*TP*$^{-/-}$, and *apoE*$^{-/-}$*IP*$^{-/-}$ mice. (**C**) Representative oil red O staining of aortic sinus sections of *apoE*$^{-/-}$ (middle), *apoE*$^{-/-}$*TP*$^{-/-}$ (lower), and *apoE*$^{-/-}$*IP*$^{-/-}$ (upper) mice. Scale bar: 200 μm. (**D**) Time course of atherosclerotic lesion development in *apoE*$^{-/-}$ (open circles), *apoE*$^{-/-}$*TP*$^{-/-}$ (filled circles), and *apoE*$^{-/-}$*IP*$^{-/-}$ (filled squares) mice. Data are means ± SEM (n = 10 for 15-week-old *apoE*$^{-/-}$ and *apoE*$^{-/-}$*IP*$^{-/-}$ and 20-week-old *apoE*$^{-/-}$ and *apoE*$^{-/-}$*TP*$^{-/-}$ male mice; n = 6 for 15-week-old *apoE*$^{-/-}$*TP*$^{-/-}$, 20-week-old *apoE*$^{-/-}$*IP*$^{-/-}$, and 30-week-old *apoE*$^{-/-}$, *apoE*$^{-/-}$*TP*$^{-/-}$, and *apoE*$^{-/-}$*IP*$^{-/-}$ mice). *P < 0.05 and **P < 0.01 versus *apoE*$^{-/-}$ mice. (**E**) Representative Sudan IV staining of en face preparations of aortas from *apoE*$^{-/-}$, *apoE*$^{-/-}$*TP*$^{-/-}$, and *apoE*$^{-/-}$*IP*$^{-/-}$ mice at 20 weeks of age. Scale bars: 2 mm. (**F**) Quantification of en face atherosclerotic lesions in *apoE*$^{-/-}$, *apoE*$^{-/-}$*TP*$^{-/-}$ and *apoE*$^{-/-}$*IP*$^{-/-}$ mice at 20 weeks of age. Data are means ± SEM (n = 5 each). *P < 0.05 and **P < 0.01 for bracketed comparisons. (**G**) Representative hematoxylin and eosin staining of innominate artery sections of *apoE*$^{-/-}$, *apoE*$^{-/-}$*TP*$^{-/-}$, and *apoE*$^{-/-}$*IP*$^{-/-}$ mice at 45 weeks of age. Scale bar: 20 μm. (**H**) Quantitative analysis of innominate atherosclerotic areas in *apoE*$^{-/-}$, *apoE*$^{-/-}$*TP*$^{-/-}$, and *apoE*$^{-/-}$*IP*$^{-/-}$ mice at 45 weeks of age. Data are means ± SEM (n = 10 each). *P < 0.05 and **P < 0.01 for bracketed comparisons.

tively expressed in most tissues and mediates basal physiological functions, while COX-2 is induced by various types of stimuli and works "on demand" in such conditions as inflammation. There is now substantial evidence that the majority of PGI_2 is produced by COX-2 in vascular ECs, whereas production of TXA_2 by platelets is catalyzed by COX-1 (10). The COX-2-catalyzed PGI_2 production probably reflects induction of COX-2 by hemodynamic shear stress in the vasculature (11). The issue of whether COX-2-derived PGI_2 exerts any protective effect on atherosclerosis is important, given that many juvenile patients with arthritis are treated with selective COX-2 inhibitors (12) and a large-scale study (VIGOR) indicated an increased tendency for cardiovascular accidents associated with the use of such drugs versus the nonselective COX inhibitor naproxen (discussed in ref. 13). Experiments examining the effects of COX-2 inhibitors in atherogenesis have yielded conflicting results. One study in which an MF-tricyclic was administered to *apoE*$^{-/-}$ mice found exaggeration of atherosclerosis (14), and one study examining the effect of rofecoxib in *LDLR*$^{-/-}$ mice detected a small but significant suppression in the development of atherosclerosis (15). The former study (14) did not specify the gender of the mice studied and may be difficult to interpret. However, two other studies, one of nimesulide in *LDLR*$^{-/-}$ mice (16) and the other of SC-236 in *apoE*$^{-/-}$ mice (17), did not find significant effects. These studies, except for the study using MF-tricyclic (14), all detected similar suppression of PGI_2 production in animals given these drugs. However, the suppression remained partial,

Table 1
Plasma cholesterol and triglyceride levels

Mouse (mg/dl)	TC (mg/dl)	TG (mg/dl)	VLDLC (mg/dl)	LDLC (mg/dl)	HDLC
C57BL/6 ($n = 8$)	99 ± 5	57 ± 4	6 ± 1	24 ± 3	58 ± 4
$TP^{-/-}$ ($n = 8$)	85 ± 9	50 ± 5	8 ± 1	19 ± 3	54 ± 4
$IP^{-/-}$ ($n = 8$)	90 ± 9	55 ± 6	7 ± 1	22 ± 3	56 ± 4
$ApoE^{-/-}$ ($n = 8$)	535 ± 43[A]	102 ± 6[A]	381 ± 36[A]	127 ± 5[A]	27 ± 4[B]
$ApoE^{-/-}TP^{-/-}$ ($n = 8$)	595 ± 53[A]	105 ± 10[A]	395 ± 60[A]	138 ± 5[A]	22 ± 4[B]
$ApoE^{-/-}IP^{-/-}$ ($n = 8$)	588 ± 52[A]	103 ± 8[A]	430 ± 44[A]	135 ± 11[A]	22 ± 4[B]

All data are shown as mean ± SEM. [A]$P < 0.01$ versus C57BL/6. [B]$P < 0.05$ versus C57BL/6.

supporting a view that both COX-1 and COX-2 contribute to PGI_2 production under pathological conditions such as atherosclerosis (3). Thus, pharmacological approaches using various drugs have produced variable and inconclusive results and have failed to provide a cohesive picture on the contribution of prostanoids, including PGI_2 and TXA_2, to atherogenesis. This probably reflects the inherent limitations associated with pharmacological studies, such as differences in the potency and specificity of individual drugs and differences in the experimental protocols and animal models. Moreover, it is difficult in principle to evaluate contribution of each prostanoid by the use of COX inhibitors, because each isoform is capable of producing more than one type of prostanoid in a variety of tissues. For example, TXA_2 is produced not only by COX-1 in blood platelets but also by COX-2 in macrophages, which is also believed to produce PGE_2 in atheromatous plaques. The importance of COX-2 in macrophages was suggested by the reduction in atherogenesis found in $LDLR^{-/-}$ mice reconstituted with $COX\text{-}2^{-/-}$ fetal liver cells (15).

In order to conquer these limitations, we have examined the development of atherosclerosis in mice deficient in prostanoid receptors for individual molecules (TXA_2 and PGI_2). TXA_2 and PGI_2 xert their effects through interaction with cell surface receptors specific to each molecule, TP and the PGI receptor (IP), respectively (18). These receptors are encoded by distinct genes and are expressed differentially in the body. With the use of homologous recombination, we have generated mice that lack either TP or IP individually and have subjected the mice to models of various diseases to analyze the roles of TXA_2 and PGI_2 (19–29). In this work, we have cross-bred TP- and IP-deficient ($TP^{-/-}$ and $IP^{-/-}$) mice with $apoE^{-/-}$ mice and have analyzed the roles played by TXA_2 and PGI_2 in atherosclerotic lesion development.

Results

Generation and lipid profile of $apoE^{-/-}TP^{-/-}$ and $apoE^{-/-}IP^{-/-}$ double-KO mice. $TP^{-/-}$ and $IP^{-/-}$ mice that had been backcrossed to the C57BL/6 background 10 times each were bred with $apoE^{-/-}$ mice that had been backcrossed to the C57BL/6 background 5 times. The resultant heterozygous mice, $apoE^{+/-}TP^{+/-}$ or $apoE^{+/-}IP^{+/-}$ mice, were cross-bred with each other, and compound mice deficient in both apoE and TP or both apoE and IP were generated. The genes encoding IP and apoE are both located on chromosome 7, with a genetic interval of approximately 1.5 cM. To generate recombination between the genes encoding IP and apoE, we mated pairs of $apoE^{+/-}IP^{+/-}$ double-heterozygous mice and selected offspring null either for *apoE* or *IP* (about 1% of the offspring) and cross-bred them with each other. Loss of TP or IP was assessed by PCR analysis (Figure 1, A and B) and was confirmed by examination of the platelet response to a TP or IP agonist (data not shown). The TP agonist I-BOP induced aggregation of platelets from $apoE^{-/-}$ mice but not of platelets from $apoE^{-/-}TP^{-/-}$ mice, whereas thrombin-induced aggregation occurred similarly in platelets from $apoE^{-/-}$ and $apoE^{-/-}TP^{-/-}$ mice. In contrast, the IP agonist cicaprost inhibited I-BOP–induced platelet aggregation in $apoE^{-/-}$ mice and this response was lost in $apoE^{-/-}IP^{-/-}$ platelets. The apoE deficiency in these mice was verified by measurement of plasma cholesterol levels and PCR analysis. At 20 weeks of age, $apoE^{-/-}TP^{-/-}$ and $apoE^{-/-}IP^{-/-}$ mice showed elevated levels of both total cholesterol (TC) and total triglyceride (TG) similar to those seen in $apoE^{-/-}$ mice (Table 1). Moreover, VLDL-cholesterol (VLDLC), LDL-cholesterol (LDLC), and HDL-cholesterol (HDLC) in $apoE^{-/-}$, $apoE^{-/-}TP^{-/-}$, and $apoE^{-/-}IP^{-/-}$ mice were almost identical. These findings suggest that loss of either TP or IP did not affect the hypercholesterolemia induced by apoE deficiency. $apoE^{-/-}TP^{-/-}$ and $apoE^{-/-}IP^{-/-}$ mice were fertile and apparently healthy. All animals were maintained on a normal chow diet and gained weight in a similar manner (data not shown).

Atherosclerotic lesion development in $apoE^{-/-}TP^{-/-}$ and $apoE^{-/-}IP^{-/-}$ mice. We used male mice of the three strains ($apoE^{-/-}$, $apoE^{-/-}TP^{-/-}$, and $apoE^{-/-}IP^{-/-}$) and examined atherosclerotic lesion development by analysis of cross-sections of the proximal aorta, en face analysis of the total aorta, and analysis of cross-sections of the innominate artery. The cross-sectional analysis of the proximal aorta was performed in the first 360 μm of the aortas of $apoE^{-/-}$, $apoE^{-/-}TP^{-/-}$, and $apoE^{-/-}IP^{-/-}$ mice at 15, 20, and 30 weeks of age. Typical oil red O staining in each strain of mice at the respective age is shown in Figure 1C. The quantitative analysis revealed significant acceleration and delay of lesion development in $apoE^{-/-}IP^{-/-}$ and $apoE^{-/-}TP^{-/-}$ mice, respectively, compared with that in $apoE^{-/-}$ mice (Figure 1D). At 15 and 20 weeks of age, the lesion areas of $apoE^{-/-}IP^{-/-}$ mice (0.206 ± 0.016 mm^2 and 0.420 ± 0.017 mm^2) were augmented significantly by 131% and 45%, respectively, compared with those of $apoE^{-/-}$ mice (0.089 ± 0.015 mm^2 and 0.290 ± 0.015 mm^2; $P < 0.05$, Tukey's t test following one-way ANOVA) (Figure 1D). After 20 weeks, lesion development in $apoE^{-/-}IP^{-/-}$ mice appeared to quickly reach a plateau and did not show a significant difference compared with that in $apoE^{-/-}$ mice at 30 weeks of age. In contrast, $apoE^{-/-}TP^{-/-}$ mice showed significant delay in the lesion development; their lesion areas at 20 and 30 weeks of age (0.087 ± 0.015 mm^2 and 0.183 ± 0.034 mm^2) were significantly suppressed, by 70% and 58%, respectively, compared with those of $apoE^{-/-}$ mice (0.290 ± 0.015 mm^2 and 0.438 ± 0.025 mm^2; $P < 0.01$, Tukey's t test following one-way ANOVA) (Figure 1D).

$ApoE^{-/-}IP^{-/-}$ and $apoE^{-/-}TP^{-/-}$ mice showed enhancement and suppression, respectively, of atherogenesis not only locally in the aortic sinus but also globally throughout aorta. En face analysis of aortic preparations of mice at 20 weeks of age revealed significant augmentation and reduction in atherosclerotic area in $apoE^{-/-}IP^{-/-}$ and $apoE^{-/-}TP^{-/-}$ mice, respectively, compared with that of $apoE^{-/-}$ mice (Figure 1E); the average lesion size in $apoE^{-/-}TP^{-/-}$ mice ($2.8\% \pm 0.4\%$) was reduced 71% compared with that in $apoE^{-/-}$ mice ($9.6\% \pm 0.9\%$; $P < 0.01$, Tukey's t test following one-way ANOVA), while that in

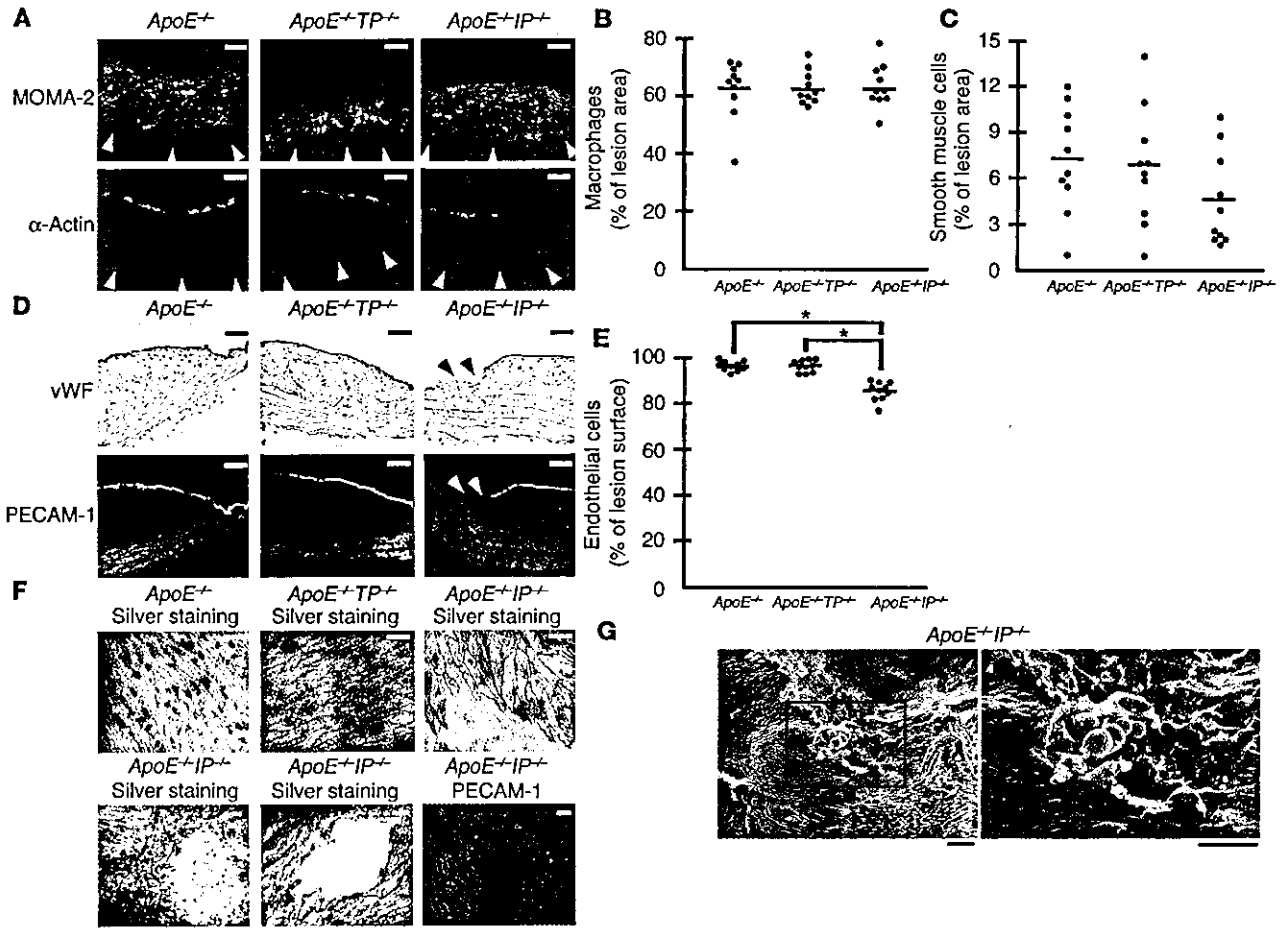

Figure 2

Effects of TP or IP deficiency on the abundance of macrophages and SMCs and EC integrity in aortic arch lesions of apoE-deficient mice at 20 weeks of age. (**A**) Representative immunostaining of macrophages and SMCs in aortic arch lesions of *apoE*$^{-/-}$ (left panels), *apoE*$^{-/-}$*TP*$^{-/-}$ (middle panels), and *apoE*$^{-/-}$*IP*$^{-/-}$ (right panels) mice. Lesions were stained with specific antibodies for macrophages (MOMA-2; upper) and for SMCs (α-actin; lower). White arrowheads indicate the external elastic lamina. Scale bars: 20 μm. (**B** and **C**) Quantitative analysis of the abundance of macrophages (**B**) and SMCs (**C**) in aortic arch lesions of *apoE*$^{-/-}$, *apoE*$^{-/-}$*TP*$^{-/-}$, and *apoE*$^{-/-}$*IP*$^{-/-}$ mice. Data are means ± SEM (n = 10 each). (**D**) Representative immunostaining of ECs in aortic arch lesions of *apoE*$^{-/-}$ (left panels), *apoE*$^{-/-}$*TP*$^{-/-}$ (middle panels), and *apoE*$^{-/-}$*IP*$^{-/-}$ (right panels) mice. Cross-sections were stained with specific antibodies for ECs (vWF, upper, and PECAM-1, red, lower) and SMCs (α-actin, green, lower). Black and white arrowheads indicate the site of endothelial disruption. Scale bars: 20 μm. (**E**) Quantitative analysis for endothelial integrity in aortic arch lesions of *apoE*$^{-/-}$, *apoE*$^{-/-}$*TP*$^{-/-}$, and *apoE*$^{-/-}$*IP*$^{-/-}$ mice by measurement of the vWF-positive signals overlying aortic lesions. Data are means ± SEM (n = 10 each). *P < 0.05 for bracketed comparisons. (**F**) Representative en face staining of aortic arch lesions of *apoE*$^{-/-}$, *apoE*$^{-/-}$*TP*$^{-/-}$, and *apoE*$^{-/-}$*IP*$^{-/-}$ mice. En face staining of aortic arch lesions with silver nitrate or anti–PECAM-1 was performed. Scale bars: 10 μm. (**G**) Representative scanning electron micrographs of aortic arches of *apoE*$^{-/-}$*IP*$^{-/-}$ mice. The right panel shows a higher magnification of the boxed area in the left panel. Scale bars: 50 μm.

apoE$^{-/-}$*IP*$^{-/-}$ mice (12.3% ± 1.0%) was augmented 28% compared with that in *apoE*$^{-/-}$ mice (P < 0.05, Tukey's t test following one-way ANOVA) (Figure 1F). Atherosclerotic lesions in *apoE*$^{-/-}$ mice were seen in the lesser curvature of the aortic arch and at the ostium of the brachiocephalic artery as well as in the abdominal aorta. The lesions in *apoE*$^{-/-}$*TP*$^{-/-}$ at this age were limited mostly to the aortic arch region, where the extent was much less. In contrast, atherosclerotic lesions in *apoE*$^{-/-}$*IP*$^{-/-}$ mice were more extensive than in *apoE*$^{-/-}$ mice in every region examined (Figure 1E).

Although analysis of atherogenesis in *apoE*$^{-/-}$ mice is carried out mostly in the aorta, atherosclerotic lesions in this strain of mice are not limited to the aorta. We noted the atherosclerotic lesion at the ostium of the brachiocephalic (innominate) artery in our en face analysis of 20-week-old mice described above. Recently, Rosenfeld et al. (30) examined the distribution of atherosclerotic lesions throughout the arterial tree of *apoE*$^{-/-}$ mice and found a highly advanced, clinically significant lesion in the innominate artery in mice 30–60 weeks of age. We therefore examined atherosclerotic lesion development in the innominate artery by cross-sectional analysis in *apoE*$^{-/-}$, *apoE*$^{-/-}$*TP*$^{-/-}$, and *apoE*$^{-/-}$*IP*$^{-/-}$ mice 45 weeks of age. As shown in the hematoxylin and eosin staining in Figure 1G, the lesion was found in all three strains of mice but the extent differed significantly. Whereas the plaques protruded into the arterial lumen only partially in *apoE*$^{-/-}$ and *apoE*$^{-/-}$*TP*$^{-/-}$ mice, those in

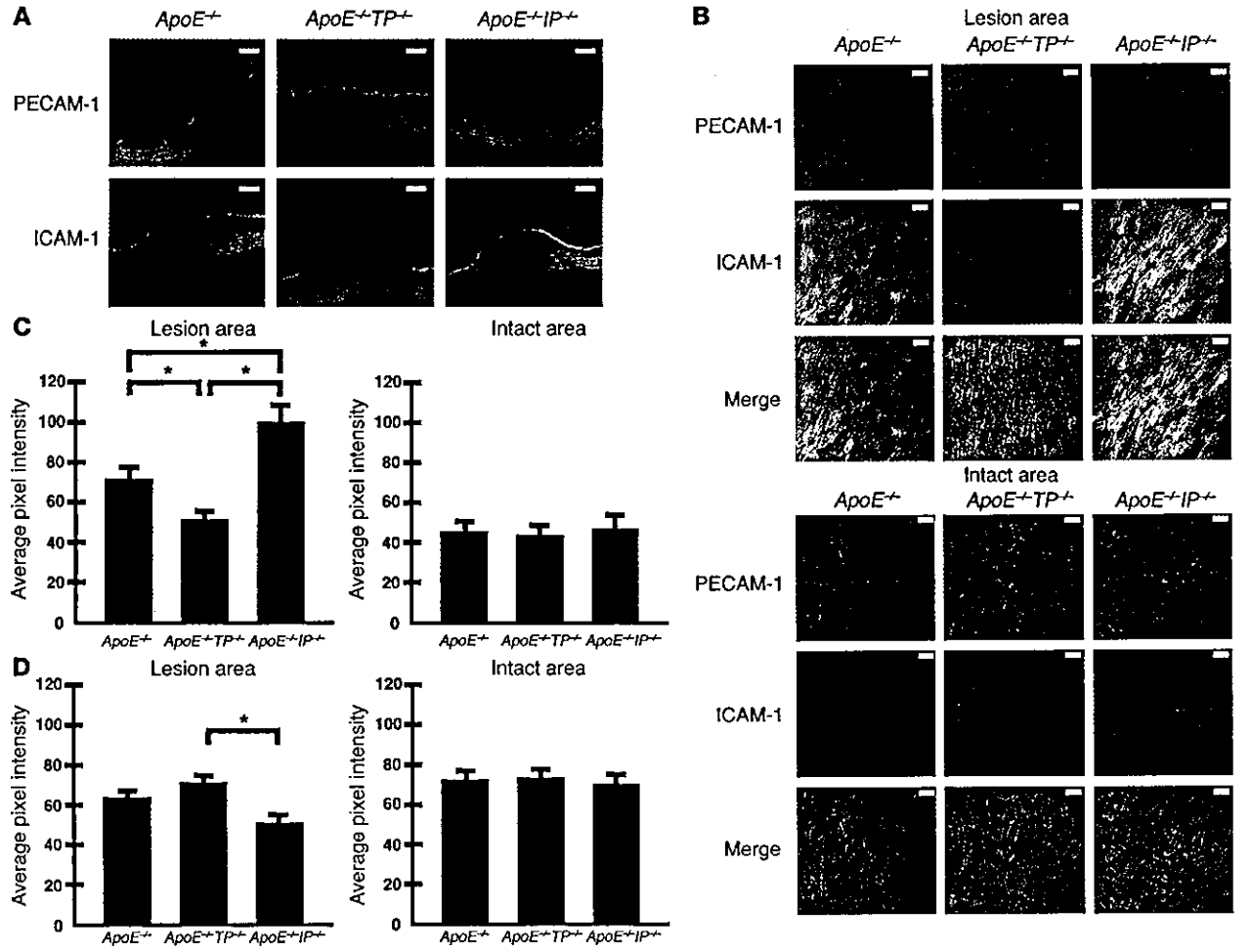

Figure 3

Effects of TP or IP deficiency on ICAM-1 and PECAM-1 expression in the ECs overlying atheromatous lesions of apoE-deficient mice. (**A**) Representative immunostaining for ICAM-1 and PECAM-1 in cross-sections from *apoE*$^{-/-}$ (left panels), *apoE*$^{-/-}$*TP*$^{-/-}$ (middle panels), and *apoE*$^{-/-}$*IP*$^{-/-}$ (right panels) mice. Mice were sacrificed at 20 weeks of age. Cross-sections were stained with specific antibodies against ICAM-1 (red; lower panels), PECAM-1 (red; upper panels), and smooth muscle α-actin (green). Scale bars: 20 μm. (**B**) Representative immunostaining of aortic arch lesions and neighboring intact areas for ICAM-1 and PECAM-1 in en face preparations of *apoE*$^{-/-}$ (left panels), *apoE*$^{-/-}$*TP*$^{-/-}$ (middle panels) and *apoE*$^{-/-}$*IP*$^{-/-}$ (right panels) mice. En face preparations were stained with specific antibodies against ICAM-1 (middle panels) and PECAM-1 (upper panels). Mice were sacrificed at 20 weeks of age. Scale bars: 10 μm. Merge, merged images. (**C** and **D**) Quantification of ICAM-1 (**C**) and PECAM-1 (**D**) expression in ECs overlying aortic arch lesions and neighboring intact areas of *apoE*$^{-/-}$, *apoE*$^{-/-}$*TP*$^{-/-}$, and *apoE*$^{-/-}$*IP*$^{-/-}$ mice. Data are means ± SEM (n = 8 each). $^{*}P < 0.05$ and $^{**}P < 0.01$ for bracketed comparisons.

apoE$^{-/-}$*IP*$^{-/-}$ mice grew extensively to partially occlude the lumen. Quantitative analysis revealed significant acceleration and delay in lesion development, respectively, in *apoE*$^{-/-}$*IP*$^{-/-}$ and *apoE*$^{-/-}$*TP*$^{-/-}$ mice compared with *apoE*$^{-/-}$ mice (Figure 1H).

Impaired EC integrity in atheromatous plaques of apoE$^{-/-}$*IP*$^{-/-}$ *mice.* To investigate whether loss of TP or IP signaling had any effect on the cell composition in atheromatous plaques, we stained macrophages, SMCs, and ECs in the plaques at the aortic arches of 20-week-old mice with antibodies against the respective marker proteins. Quantification of macrophage and SMC abundance in the plaques and of endothelial integrity on the lesion surface was performed on the ten sections taken every 18 μm as described in Methods (Figure 2). Cells staining positive for MOMA-2 were found throughout the plaques in all of *apoE*$^{-/-}$, *apoE*$^{-/-}$*TP*$^{-/-}$, and *apoE*$^{-/-}$*IP*$^{-/-}$ mice at this stage. Quantification revealed that MOMA-2-stained cells occupied about 60% of the total plaque area and there were no significant differences among the three strains (Figure 2, A and B). The fact that the area inside the plaque was stained homogenously with oil red O suggested that these MOMA-2-positive cells represented macrophage-derived foam cells and the space not occupied by macrophages represented mostly lipid cores. SMCs staining positive for α-actin accumulated and formed a layer at the top of the lesion beneath the EC layer (Figure 2A and data not shown). Quantification revealed that they comprised about 7% of the total plaque area in *apoE*$^{-/-}$ and *apoE*$^{-/-}$*TP*$^{-/-}$ mice (Figure 2C). The proportion of SMCs in *apoE*$^{-/-}$*IP*$^{-/-}$ mice tended to be lower than that in the other two strains of mice, but there was no significant difference. This SMC phenotype of *apoE*$^{-/-}$*IP*$^{-/-}$ mice is at odds with the suppression

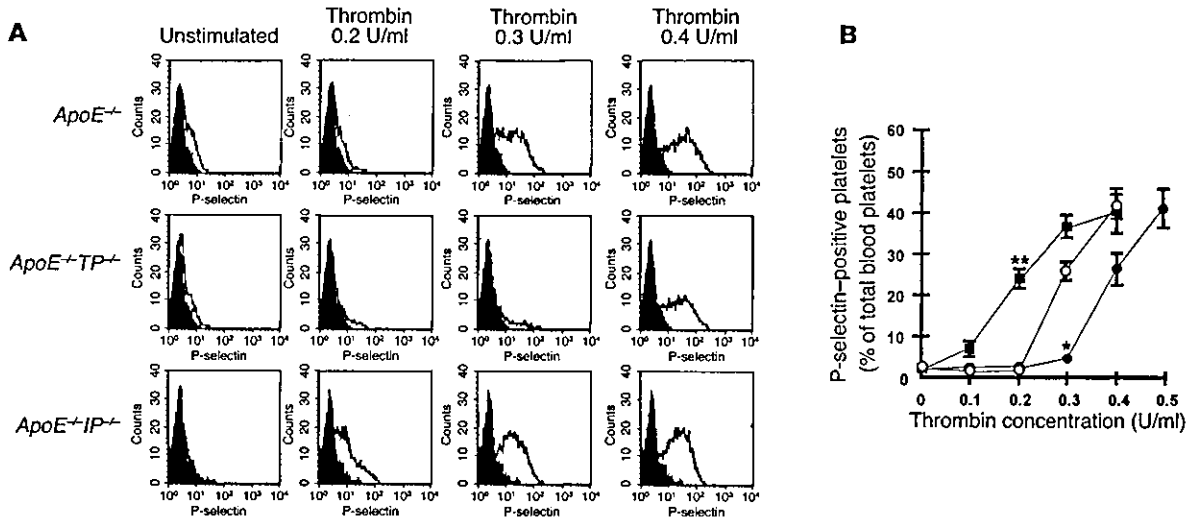

Figure 4

Platelet reactivity for thrombin-induced surface expression of P-selectin. (**A**) Representative histograms of thrombin-induced P-selectin expression in platelets from *apoE*$^{-/-}$ (upper panels), *apoE*$^{-/-}$*TP*$^{-/-}$ (middle panels), and *apoE*$^{-/-}$*IP*$^{-/-}$ (lower panels) mice. Platelets were either left unstimulated or were stimulated with 0.2, 0.3, or 0.4 U/ml of thrombin. They were then labeled with FITC-conjugated anti–P-selectin and were analyzed by flow cytometry. Filled histograms indicate background signal. (**B**) Quantification analysis. Concentration-dependent effect of thrombin for P-selectin expression was determined in platelets from *apoE*$^{-/-}$ (open circles), *apoE*$^{-/-}$*TP*$^{-/-}$ (filled circles), and *apoE*$^{-/-}$*IP*$^{-/-}$ (filled squares) mice. Data are means ± SEM (n = 9 each). $^{*}P < 0.05$ and $^{**}P < 0.01$ versus *apoE*$^{-/-}$ mice.

of SMC proliferation by a PGI_2 analog (cicaprost) in vitro (22) as well as the enhanced proliferative response found in IP-deficient mice subjected to chronic hypoxia (23) or catheter-induced carotid vascular injury (31). Impaired SMC proliferation in the absence of IP may suggest that SMC proliferation is under more complex regulation in atherosclerosis or that it may be unique to the apoE-deficient mice. These points should be clarified in future studies.

EC integrity on the plaque surface was then examined by staining of the cross-sections for two endothelial markers: von Willebrand factor (vWF) and platelet endothelial cell adhesion molecule 1 (PECAM-1). As expected, the staining was seen as a linear signal in the EC layer over the plaques. There was occasional loss of staining of these two markers in the plaques of *apoE*$^{-/-}$*IP*$^{-/-}$ mice, especially on the "shoulder" of atherosclerotic lesions (Figure 2D). In contrast, no such irregularity in EC staining on the plaque surface was seen in *apoE*$^{-/-}$ and *apoE*$^{-/-}$*TP*$^{-/-}$ mice. Quantification of vWF staining on the plaque surface revealed a significant reduction in *apoE*$^{-/-}$*IP*$^{-/-}$ mice (85.5% ± 0.7%) compared with *apoE*$^{-/-}$ mice (98.0% ± 0.5%, $P < 0.05$, Tukey's t test following one-way ANOVA) and *apoE*$^{-/-}$*TP*$^{-/-}$ mice (98.5% ± 0.5 %, $P < 0.05$, Tukey's t test following one-way ANOVA) (Figure 2E). Compatible with these findings in the cross-sections, staining of en face preparations with silver nitrate as well as anti-PECAM revealed loss of ECs which was consistently associated with the "shoulder" of a plaque in *apoE*$^{-/-}$*IP*$^{-/-}$ mice (Figure 2F). Such EC loss was rarely seen in *apoE*$^{-/-}$ and *apoE*$^{-/-}$*TP*$^{-/-}$ mice (observations of 5 mice of each strain). Scanning electron microscopy of the aortic arch region revealed again focal endothelial disruption in the "shoulder" of atheromatous plaques of all of three *apoE*$^{-/-}$*IP*$^{-/-}$ mice examined, while none of three *apoE*$^{-/-}$ or *apoE*$^{-/-}$*TP*$^{-/-}$ mice showed such lesions. In some cases, the lesion of endothelial disruption formed a crater in which monocyte/macrophage-like cells accumulated (Figure 2G). These findings suggest that the EC loss had already occurred in vivo and was not an artifact created during sample preparation.

ICAM-1 and PECAM-1 expression on ECs in apoE$^{-/-}$*TP*$^{-/-}$ *and apoE*$^{-/-}$*IP*$^{-/-}$ *mice.* To explore endothelium activation in *apoE*$^{-/-}$*TP*$^{-/-}$ and *apoE*$^{-/-}$*IP*$^{-/-}$ mice, we stained for ICAM-1 and PECAM-1 in ECs overlying the lesions of the three lines of mice. In cross-sections, PECAM-1 expression was found more or less homogenously through the EC monolayer overlying the lesions, while ICAM-1 expression by endothelium was most intense at borders and the "shoulder" of the lesions in all of the three strains of mice (Figure 3A). We then performed quantitative analysis using en face confocal microscopy images (Figure 3B). In the ECs overlying the lesions, *apoE*$^{-/-}$*TP*$^{-/-}$ mice had a significant decrease in ICAM-1 expression (53.9 ± 1.8 versus 73.1 ± 4.1; $P < 0.05$, Tukey's t test following one-way ANOVA; values measured in arbitrary units based on fluorescence intensity per pixel) compared with that of *apoE*$^{-/-}$ mice, whereas ICAM-1 expression in *apoE*$^{-/-}$*IP*$^{-/-}$ mice significantly increased (100.5 ± 7.6; $P < 0.01$, Tukey's t test following one-way ANOVA) (Figure 3C). In contrast, there was no difference in ICAM-1 expression in ECs in intact areas among the three strains of mice, which was low compared with that in the atherosclerotic lesions. As for PECAM-1 expression in the atherosclerotic lesions, expression in *apoE*$^{-/-}$*TP*$^{-/-}$ mice or *apoE*$^{-/-}$*IP*$^{-/-}$ mice tended to increase or decrease, respectively, compared with that in *apoE*$^{-/-}$ mice, and there was a significant difference in expression between *apoE*$^{-/-}$*IP*$^{-/-}$ and *apoE*$^{-/-}$*TP*$^{-/-}$ mice (52.4 ± 3.2 versus 68.3 ± 1.7; $P < 0.05$, Tukey's t test following one-way ANOVA) (Figure 3D). There was also no difference in PECAM-1 expression in the ECs of intact areas among the three strains of mice.

Reactivity of platelets in apoE$^{-/-}$, *apoE*$^{-/-}$*TP*$^{-/-}$, *and apoE*$^{-/-}$*IP*$^{-/-}$ *mice.* Because TXA_2 and PGI_2 are potent activators and suppressors, respectively, of blood platelets, chronic loss of their actions may cause alterations in platelet reactivity to an aggregating agent. Reactivity of blood platelets was therefore compared among *apoE*$^{-/-}$, *apoE*$^{-/-}$*TP*$^{-/-}$, and *apoE*$^{-/-}$*IP*$^{-/-}$ mice by whole-blood flow cytometry (32, 33). Briefly,

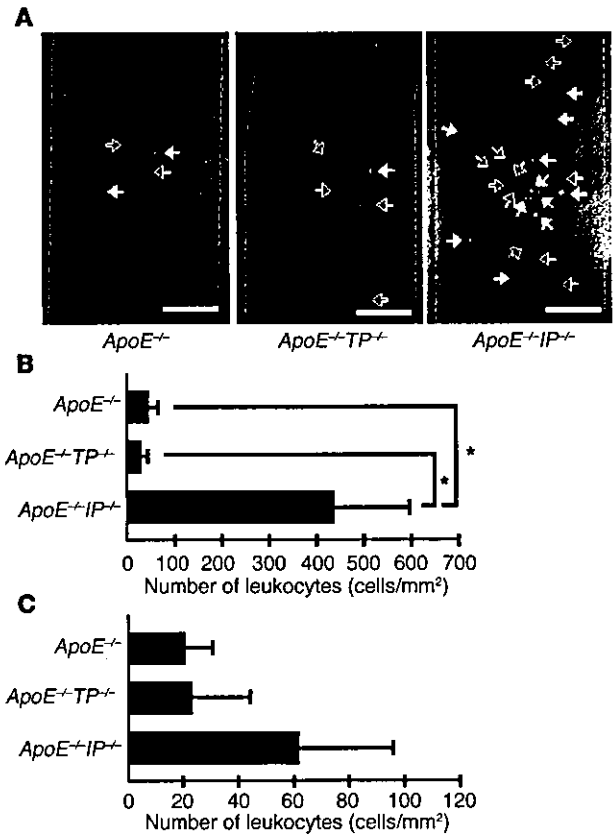

Figure 5
Intravital microscopy for leukocyte rolling and adhesion. (**A**) Fluorescence images of rolling and adherent leukocytes. Black and white arrows indicate rolling and adherent leukocytes, respectively. Vessel lumens are outlined by broken lines. Scale bars: 0.1 mm. (**B**) Quantitative analysis of rolling leukocytes. Data are means ± SEM ($n = 5$ each). *$P < 0.05$ versus $apoE^{-/-}$ and $apoE^{-/-}TP^{-/-}$ mice. (**C**) Quantitative analysis for adherent leukocytes as described in **B**.

diluted blood was activated with various concentrations of thrombin and expression of P-selectin on the platelet surface was evaluated by flow cytometry. Expression of P-selectin was barely detected on unstimulated platelets, but the number of blood platelets showing surface P-selectin expression increased with increasing concentrations of thrombin. P-selectin expression was induced significantly with 0.3 U/ml thrombin and increased with 0.4 U/ml thrombin on the platelets of $apoE^{-/-}$ mice (Figure 4, A and B), whereas its expression was only marginally induced at 0.3 U/ml thrombin in the platelets of $apoE^{-/-}TP^{-/-}$ mice (Figure 4, A and B). In contrast, an increase in the P-selectin expression was detected at doses as low as 0.1 U/ml and increased significantly with 0.2 U/ml thrombin in the platelets of $apoE^{-/-}IP^{-/-}$ mice (Figure 4, A and B). These results indicate that the platelets of $apoE^{-/-}TP^{-/-}$ and $apoE^{-/-}IP^{-/-}$ mice have lower and higher sensitivity to thrombin, respectively, than those of $apoE^{-/-}$ mice.

Leukocyte adherence in the common carotid arteries of $apoE^{-/-}IP^{-/-}$ mice. Finally, we examined the leukocyte-EC interaction by intravital microscopy. Rhodamine 6G was injected i.v. into $apoE^{-/-}$, $apoE^{-/-}TP^{-/-}$, and $apoE^{-/-}IP^{-/-}$ mice to label leukocytes in vivo, and interaction of the leukocytes with the wall of the common carotid artery was examined by intravital microscopy. Leukocytes rolling or adhering were seen as fluorescent dots on the wall of the artery (Figure 5A). Quantitative analysis revealed a significantly greater number of leukocytes rolling on the walls of arteries in $apoE^{-/-}IP^{-/-}$ mice than in either $apoE^{-/-}$ or $apoE^{-/-}TP^{-/-}$ mice (Figure 5B). Additionally, adhesion of leukocytes also tended to be higher in $apoE^{-/-}IP^{-/-}$ mice (Figure 5C). Although rhodamine 6G also labeled platelets, we did not see thrombus formation or detachment in any strain of mice during our observation period.

Discussion

TXA_2 and PGI_2 are two major prostanoids in the cardiovascular system, being abundantly produced by blood platelets and vascular endothelium, respectively. Previous studies found that TXA_2 and PGI_2 biosynthesis is increased in patients with atherosclerosis (2, 3). In this work, we generated compound mice, $apoE^{-/-}TP^{-/-}$ and $apoE^{-/-}IP^{-/-}$, and examined the roles of TXA_2 and PGI_2 in the initiation and progression of atherosclerosis. $ApoE^{-/-}$ mice develop a spectrum of atherosclerotic lesions similar to that of humans (34). They also show elevated production of TXA_2 and PGI_2, as seen in humans (35). Thus, the $apoE^{-/-}$ mouse is a suitable animal model for evaluation of the roles of TXA_2 and PGI_2 in atherosclerosis. Previously, the involvement of these prostanoids in atherosclerosis was examined by the use of various COX inhibitors in this and similar animal models. However, the results obtained by those studies were variable (7, 8, 14–17). In addition, a study using a TP antagonist in $apoE^{-/-}$ mice showed only a marginal reduction in atherogenesis (8). In contrast to those findings in the previous studies, our study here using genetically engineered mice has demonstrated significant suppression and significant enhancement of atherosclerosis in $apoE^{-/-}TP^{-/-}$ and $apoE^{-/-}IP^{-/-}$ mice, respectively, suggesting strongly proatherogenic and antiatherogenic actions of TXA_2 and PGI_2, respectively. TP deficiency suppressed the extent of atherosclerosis at both 20 and 30 weeks of age. Suppression of atherosclerosis by TP deficiency is much more robust (70% at 20 weeks of age and 58% at 30 weeks of age) than that found after treatment with the TP antagonist S-18886 (about 20%) (8). We have also examined the effects of TP or IP deficiency on the development of vascular lesions in the innominate arteries of 45-week-old $apoE^{-/-}$ mice. Rosenfeld et al. (30) previously noted more-advanced vascular lesions in the innominate arteries in $apoE^{-/-}$ mice. In this study we have not only confirmed their findings in $apoE^{-/-}$ mice but also found that this lesion was far more advanced in $apoE^{-/-}IP^{-/-}$ mice, whereas the disease progression appeared to be retarded in $apoE^{-/-}TP^{-/-}$ mice.

It is noteworthy that atherogenesis was significantly accelerated and reached a plateau early in $apoE^{-/-}IP^{-/-}$ mice compared with $apoE^{-/-}$ mice. These results indicate that signaling from PGI_2 to IP is important in preventing the initiation of atherosclerosis. Impaired PGI_2 function, moreover, appeared to affect the progression and nature of atherosclerotic plaques. Our analysis detected frequent loss of ECs in the plaques of $apoE^{-/-}IP^{-/-}$ mice. In addition to ECs, we also found that the abundance of SMCs tended to be lower in the plaques of $apoE^{-/-}IP^{-/-}$ mice (Figure 2). Lesions with impaired EC integrity and weaker fibrous caps are suggested to be prone to rupture (36). Recently, Cipollone and colleagues found that COX-2 and membrane-bound PGE synthetase are upregulated in macrophages in atheromatous plaques of humans and induce expression of matrix metalloproteinase-9 and proposed that this pathway leads to plaque instability (37, 38). It is interesting in this context that PGI_2 can suppress expression of

this matrix metalloproteinase isoform in vitro and in vivo (39, 40). Lesion rupture, when it occurs in vivo, then precipitates thrombosis, which is further accelerated in the absence of IP. Disruption of IP is known to increase the risk of thrombosis (20). Thus, PGI_2 appears to exert important inhibitory actions on the initiation and progression of atherosclerosis, and the reduction in PGI_2 in the presence of normal TXA_2 formation is likely to lead an increased risk of atherosclerosis and thrombosis. Currently, an important question concerning COX-2 inhibitors is whether the selective reduction in PGI_2 increases the risk of atherosclerosis. Our findings support that conclusion. However, our findings cannot be directly extrapolated to the clinical outcome of patients treated with COX-2 inhibitors. Although the majority of PGI_2 under basal conditions is derived from COX-2 catalysis, both COX-1 and COX-2 contribute to the increase in PGI_2 in patients with atherosclerosis as well as in *apoE*$^{-/-}$ mice (3, 17), and selective inhibition of COX-2 usually results in only partial inhibition of PGI_2 production (15–17). In addition, TXA_2 can be derived also from COX-2 in atherosclerotic plaques. COX-2 is expressed by monocytes/macrophages in mouse atherosclerotic lesions (15). Macrophages contain TX synthase and release large amounts of TXA_2 when transformed into foam cells with modified LDL (41).

What, then, are the underlying mechanisms of the actions of TXA_2 and PGI_2 in atherogenesis? Activation and inhibition of blood platelets by TXA_2 and PGI_2, respectively, may certainly be one of the mechanisms. Activated platelets were found in the circulating blood of patients with atherosclerosis (42–44) and hypercholesterolemia (45, 46). We have examined this issue by using whole-blood flow cytometry for thrombin-induced P-selectin expression in platelets (32). This method has been used frequently to evaluate platelet reactivity in patients with various cardiovascular disorders (33). Our analysis has revealed that platelets of *apoE*$^{-/-}$*TP*$^{-/-}$ and *apoE*$^{-/-}$*IP*$^{-/-}$ mice have lower and higher reactivity, respectively, than those of *apoE*$^{-/-}$ mice, which is consistent with the atherosclerotic phenotypes observed in the three strains of mice.

Here, we have further examined effects of TP or IP disruption on expression of adhesion molecules on ECs. Adhesion molecules on ECs play important roles in the migration of monocytes/macrophages through the EC monolayer and the initiation of atheromatous plaques. Indeed, ICAM-1 is strongly expressed in atherosclerotic plaques of humans (47) and the level of soluble ICAM-1 correlates with the severity of atherosclerosis (48). In *apoE*$^{-/-}$ mice, ICAM-1 expression is high in atherosclerosis-prone sites of the aorta, and deficiency in ICAM-1 in apoE-deficient mice significantly reduces atherosclerotic lesions (49). We have found that ICAM-1 expression on ECs overlying the plaques of *apoE*$^{-/-}$*TP*$^{-/-}$ mice is significantly lower, while that of *apoE*$^{-/-}$*IP*$^{-/-}$ mice is significantly higher, than ICAM-1 expression in *apoE*$^{-/-}$ mice (Figure 3). The changes in the ICAM-1 expression in the presence of TP or IP deficiency are consistent with the reported in vitro actions of TXA_2 and PGI_2. ICAM-1 expression is induced by proinflammatory cytokines from activated macrophages such as TNF-α or IL-1β (50). Signaling from PGI_2 to IP is known to inhibit TNF-α production by activated macrophages (21) and to reduce IL-1–induced ICAM-1 expression on ECs (51). In contrast, stimulation of TP induces ICAM-1 expression in cultured ECs in vitro (52, 53), suggesting that TXA_2 formed in situ in atheromatous plaques acts on ECs to induce ICAM-1 expression to amplify atherogenesis. Interestingly, TXA_2 and PGI_2 appear to have effects opposite to those of ICAM-1 on the expression of PECAM-1 on the plaque ECs, which was up- and downregulated in *apoE*$^{-/-}$*TP*$^{-/-}$ and *apoE*$^{-/-}$*IP*$^{-/-}$ mice, respectively. PECAM-1 was first described as an adhesion molecule essential in the transmigration of leukocytes through endothelial monolayer (54). However, recent analyses of *PECAM-1*$^{-/-}$ mice in various models showed that PECAM-1 deficiency did not block but instead enhanced leukocyte accumulation at inflammation sites (55–57). Given its intracellular domain, PECAM-1 is now suggested to be an inhibitory signaling molecule (58). Intriguingly, regulation of PECAM-1 expression is opposite to that of ICAM-1. For example, a previous report showed that the expression of PECAM-1 and ICAM-1 on cultured human umbilical vein ECs was down- and upregulated, respectively, after activation with TNF-α plus IFN-γ (59). Such opposite modes of expression may explain the changes in the patterns of ICAM-1 and PECAM-1 expression found in the atherosclerosis phenotypes of *apoE*$^{-/-}$*TP*$^{-/-}$ and *apoE*$^{-/-}$*IP*$^{-/-}$ mice.

The above findings on the reactivity of platelets and the expression of adhesion molecules in ECs in *apoE*$^{-/-}$, *apoE*$^{-/-}$*TP*$^{-/-}$, and *apoE*$^{-/-}$*IP*$^{-/-}$ mice suggest that TP or IP deficiency can affect the interaction of ECs with platelets and leukocytes. We examined this issue by intravital microscopy. Although we did not detect significant platelet adhesion to the blood vessels of any of the three lines of mice under basal conditions, we found significant leukocyte adherence to the wall of the common carotid artery in *apoE*$^{-/-}$*IP*$^{-/-}$ mice. This may be relevant to the higher platelet reactivity and enhanced ICAM-1 expression in this line of animals. Platelet P-selectin is suggested to play an important role in mediating the leukocyte-EC interaction (60). It may be also relevant to the EC disruption observed in *apoE*$^{-/-}$*IP*$^{-/-}$ mice.

In conclusion, using the IP-deficient and TP-deficient mice, we were able to evaluate separately the contributions of PGI_2 and TXA_2 to the development of atherosclerosis. The information presented here will aid in the interpretation of clinical findings and the evaluation of risk in atherosclerotic patients treated with various drugs modulating the arachidonate cascade. Our findings also indicate that the administration of PGI mimetics and TP antagonists may be useful in the prevention of atherosclerosis. This line of genetic approach may also help to identify the contributions of PGs other than PGI_2 and TXA_2 to atherosclerosis.

Methods

Generation of apoE$^{-/-}$*TP*$^{-/-}$ *and apoE*$^{-/-}$*IP*$^{-/-}$ *double-KO mice.* *ApoE*$^{-/-}$ mice (129Ola × C57BL/6 mixed background) were a generous gift from Edward M. Rubin (University of California at Berkeley, Berkeley, California, USA) (4). Mice lacking TP or IP individually were generated as described (19, 20). *ApoE*$^{-/-}$, *TP*$^{-/-}$, and *IP*$^{-/-}$ mice were backcrossed 5, 10, and 10 times, respectively, to C57BL/6CrSlc mice (Japan SLC). *TP*$^{-/-}$ and *IP*$^{-/-}$ mice were then cross-bred with *apoE*$^{-/-}$ mice. Functional disruption of the gene encoding apoE was confirmed by markedly elevated plasma cholesterol levels. Genotype analyses of *apoE*$^{-/-}$, *TP*$^{-/-}$, and *IP*$^{-/-}$ mice were performed by PCR using genomic DNA isolated from tail snip samples as a template. PCR analysis was performed for apoE alleles with the sense primers exon2 (5′-GTGCTGTTGGTCACATTGCTGACA-3′) and Neo1 (5′-ATGGGATCGGCCATTGAACA-3′) for WT and mutant alleles, respectively, and the antisense primer exon3 (5′-TCAGTTCTTGTGTGACTTGGGAGC-3′); for TP alleles with the sense primers ML139 (5′-ACTTTGTTGCAGACACCACCTGTC-3′) and Neo2 (5′-TGATATTGCTGAAGAGCTTGGCGGCGA-3′) for WT and mutant alleles, respectively, and the antisense primer ML136 (5′-AAGCTTGGGTTTCAGGGACCT-3′); and for IP alleles with the sense primer CY37 (5′-GTATCTTTCAGTACCTGAGGACTG-3′) and

the antisense primers CY41 (5′-GAGCAGAAAAATTCCCAGAGGCTT-3′) and Neo17 (5′-TGACCGCTTCCTCGTGCTTTAC-3′) for WT and mutant alleles, respectively (Figure 1A). Reaction mixtures contained 10 mM Tris-HCl, pH 8.3, 50 mM KCl, 1.5 mM $MgCl_2$, 0.1% Triton X-100, 10% DMSO, 0.25 mM dNTPs, 20 pmol of each primer, and 1 U of Taq DNA polymerase (Toyobo) in a total volume of 20 μl. After a denaturation step at 94°C for 3 minutes, 35 cycles of the amplification step (94°C for 60 seconds, 58°C for 60 seconds, and 72°C for 80 seconds) were carried out, followed by a final elongation step of 3 minutes at 72°C. For apoE alleles, primers exon2 and exon3 amplify a 0.7-kb WT allele fragment, and primers Neo1 and exon3 amplify a 0.4-kb mutant allele fragment. For TP alleles, primers ML139 and ML136 amplify a 0.9-kb WT allele fragment, and primers Neo2 and ML136 amplify a 1.1-kb mutant allele fragment (Figure 1A). For IP alleles, primers CY37 and CY41 amplify a 1.3-kb WT allele fragment, and primers CY37 and Neo17 amplify a 0.9-kb mutant allele fragment (Figure 1A). Mice were kept on a 12-hour light/dark cycle and were fed a normal chow diet (F2; Funabashi Farm). Food and water were available ad libitum. All experiments were performed in male mice. All experimental procedures were approved by the Committee on Animal Research of Kyoto University Faculty of Medicine.

Preparation of mouse platelets and platelet aggregation assay. Platelet aggregation was examined as described previously (61). Blood (1.0 ml) was drawn by cardiac puncture of ether-anesthetized mice with a syringe containing 50 μl of 3.8% trisodium citrate. Blood pooled from 3–4 animals was diluted with an equal volume of modified Tyrode-HEPES buffer, pH 7.4 (20 mM HEPES, 140 mM NaCl, 5 mM $MgCl_2$, and 5 mM KCl). Platelet-rich plasma (PRP) was prepared by centrifugation at 160 *g* for 5 minutes at room temperature. Platelet-poor plasma was obtained by further centrifugation of the blood after PRP was removed at 1,500 *g* for 10 minutes at room temperature. The number of platelets in the PRP was adjusted to 3×10^5 platelets/μl. Platelet aggregation was measured with an aggregometer (NBS Hema Tracer 601; Tokyo Koden). I-BOP, a TP agonist, was used to activate platelets, and cicaprost, an IP agonist, was used to inhibit platelet aggregation.

Lipid and lipoprotein analyses. Blood (1.0 ml) was drawn by cardiac puncture of ether-anesthetized mice into a tube containing EDTA (final concentration, 5 mM). Plasma was isolated by centrifugation at 1,500 *g* for 10 minutes and was maintained at 4°C. Plasma cholesterol and triglyceride were measured using Toyobo enzymatic assay kits (Toyobo). For quantification of the cholesterol content of each lipoprotein, lipoproteins were separated at buoyant densities of 1.019 g/ml and 1.063 g/ml by ultracentrifugation. VLDLC is the difference between TC and cholesterol with a density greater than 1.019 g/ml; HDLC is cholesterol with a density of more than 1.063 g/ml cholesterol; LDLC is the difference between TC and the sum of VLDLC and HDLC.

Quantification of atherosclerosis. Atherosclerotic lesions were quantified by en face analysis of the whole aorta and by cross-sectional analysis of the proximal aorta and the innominate artery. For en face preparations of the aorta, a cannula was inserted into the left ventricle and the aortic tree was fixed by perfusion for 10 min with ice-cold PBS containing 4% paraformaldehyde (PFA), 5% sucrose, 20 μM butylated hydroxytoluene, and 2 μM EDTA, as described previously (62, 63). The aorta was opened longitudinally, from the heart to the iliac arteries, while still attached to the heart and major branching arteries in the body. The primary incision followed the ventral side of the aorta and the inner curvature of the arch. To obtain a flat preparation for imaging, a second incision was made along the outer curvature of the arch. The aorta (from the heart to the iliac bifurcation) was then removed and was "pinned out" on a black wax surface in a dissecting pan using stainless steel pins 0.2 mm in diameter. After overnight fixation with the PFA solution described above and a 12-hour rinse in PBS, the aortas were briefly rinsed in 70% ethanol; immersed for 6 minutes in a filtered solution containing 0.5% Sudan IV, 35% ethanol, and 50% acetone; and destained for 5 minutes in 80% ethanol. The Sudan IV–stained aortas were photographed and were used for quantification of atherosclerotic lesions.

For cross-sectional analysis of the aorta, hearts were isolated from mice sacrificed by cervical dislocation, were washed in PBS, and were embedded in OCT compound. The OCT-embedded hearts were sectioned with a cryostat, and 6-μm sections in the proximal aorta were obtained sequentially beginning at the aortic valve. Sections were transferred onto a Superfrost slide (Matsunami) and were stained with oil red O followed by counterstaining with hematoxylin (4). Ten sections obtained every 36 μm from the aortic sinus were used for quantification of lesion areas with Image Pro Plus software (Media Cybernetics). The average lesion area of the ten sections from each heart was taken as a value to represent that animal, and the means of the average lesion areas from each group were compared as described previously (64, 65).

Atherosclerotic lesions in the innominate artery were quantified by cross-sectional analysis. Innominate arteries were isolated from 45-week-old male mice sacrificed by cervical dislocation, were washed in PBS, and were embedded in OCT compound. OCT-embedded innominate arteries were sectioned with a cryostat and 8-μm sections were obtained sequentially. Sections were transferred onto a Superfrost slide and were stained with hematoxylin and eosin. Ten sections obtained every 80 μm were used for quantification of lesion areas with Image Pro Plus software. The average lesion area of the 10 sections from each innominate artery was taken as a value to represent that animal and the means of the average lesion areas from 10 mice were compared.

Immunohistochemistry. For cross-sectional analyses, the aortic tree was perfused with ice-cold PBS containing 5 mM EDTA via a cannula inserted into the left ventricle for 10 minutes. The aortic arch was isolated, embedded in OCT compound, and sectioned at a thickness of 6 μm with a cryostat. Sections containing atherosclerotic plaques were identified by microscopy. These sections were then fixed in 4% PFA at 4°C for 10 minutes, were immersed in PBS for 5 minutes for rehydration of the tissues, and were blocked overnight at 4°C with 2% skim milk (BD) in PBS. For evaluation of the abundance of macrophages and SMCs and the expression of ICAM-1 (CD54) and PECAM-1 (CD31) in the lesions, sections were incubated overnight at 4°C with a 1:200 dilution of rat MOMA-2 mAb against mouse macrophages (Accurate Chemical and Scientific Co.); a 1:200 dilution of mouse 1A4 mAb against human α-smooth muscle actin, labeled with FITC (Dako); a 1:200 dilution of armenian hamster mAb against mouse ICAM-1, labeled with Texas Red (BD); and a 1:200 dilution of rat mAb against mouse PECAM-1, labeled with FITC or Texas Red (BD). Sections incubated with MOMA-2 antibody were then washed and incubated with a 1:400 dilution of goat anti-rat IgG, labeled with Texas Red (BD). For vWF staining, endogenous peroxidase activity was blocked by incubation of sections at 4°C for 30 minutes with 0.3% (volume/volume) H_2O_2 in PBS. The sections were then incubated overnight at 4°C with a 1:200 dilution of mouse mAb against human vWF, labeled with HRP (Sigma-Aldrich). After a thorough washing, staining was developed with diaminobenzidine followed by counterstaining with hematoxylin. Ten sections obtained every 18 μm from aortic arch were used for quantification of the macrophages and SMCs and EC density of the lesions with Image-Pro Plus software. The macrophages and SMCs were quantified by measurement of the area that stained positive for the respective markers, as described previously (7). EC density was determined by the ratio of the vWF-positive luminal surface length to the total luminal surface length of each cross-sectional plaque. The average of the 10 sections was taken to represent 1 animal, and the means of the averages from each group were compared.

For the en face analysis, the aortic tree was first washed by perfusion with ice-cold PBS containing 5 mM EDTA and then was fixed by perfusion with ice-cold PBS containing 4% PFA via a cannula inserted into the left ventricle, each perfusion for 10 minutes. The aortic arch was isolated and opened longitudinally. En face preparations were blocked overnight at 4°C with 2% skim milk in PBS and were incubated overnight at 4°C with a 1:500 dilution of rat mAb against mouse PECAM-1, labeled with FITC, and armenian hamster mAb against mouse ICAM-1, labeled with Texas Red. Because activation of ECs occurs on the "shoulder" of plaques (66), five images (1,024 × 1,024 pixels/image) were obtained randomly from the EC monolayer on the "shoulder" of plaques with a Bio-Rad MRC-1024 confocal microscope. The average pixel intensity of the five images was taken as a value to represent that animal, and the means of the average pixel intensity from each group were compared as described previously (60).

Silver nitrate staining of en face endothelial cells. The aortic tree was washed, stained, and fixed as described previously (67, 68) by successive perfusion in the following solutions: 10 ml of 5% glucose; 4 ml of 0.25% silver nitrate; 2 ml of 5% glucose; 8 ml of 3% cobalt bromide and 1% ammonium bromide; 2 ml of 5% glucose; 4 ml of 4% PFA; 10 ml of distilled water; 2 ml of hematoxylin; and 10 ml of distilled water. The aortic arch was isolated, opened longitudinally, and mounted with the endothelium upward on a Superfrost slide.

Scanning electron microscopy. The aortic trees of 20-week-old male mice were washed at 37°C for 10 minutes with PBS and were fixed at room temperature for 10 minutes with PBS containing 1% glutaraldehyde by perfusion, as described previously (69). The aortic tree was then excised, opened longitudinally, additionally fixed by immersion in PBS containing 1% glutaraldehyde at room temperature for 24 hours, dehydrated in ethanol, and processed by critical point drying with CO_2. The aortic tree specimens were then oriented with the lumens exposed, mounted with carbon paint, and coated with gold for scanning electron microscopy (T-330; Nippon Denshi).

Flow cytometry for platelet reactivity. Platelet reactivity was examined by whole-blood flow cytometry (32, 33). Blood (1.0 ml) was drawn by cardiac puncture of ether-anesthetized mice with a syringe containing 50 μl of 3.8% trisodium citrate. Within 10 minutes of being drawn, the blood was diluted 1:4 in modified Tyrode-HEPES buffer, pH 7.4, and the diluted blood was activated at 37°C for 10 minutes with 0.1–0.5 U/ml thrombin, incubated at room temperature for 30 minutes with a 1:100 dilution of rat mAb against mouse P-selectin, labeled with FITC, and fixed at 4°C for 2 hours with ice-cold PBS containing 1% PFA. Samples were then analyzed using a FACSVantage flow cytometer (BD).

Intravital microscopy. Leukocyte-EC interaction was examined by intravital microscopy using rhodamine 6G that stained in vivo leukocytes, as described previously (29, 60, 69). Five male mice 25–30 weeks of age were used for each strain. Rhodamine 6G was injected i.v., and the numbers of leukocytes rolling on and adhering to the wall of the common carotid artery were examined "off-line" during video playback analysis. A leukocyte was defined as rolling if it migrated along the vessel wall at a rate less than 200 μm/s and as adhering if it remained stationary for more than 20 seconds. We counted the number of leukocyte rolling and adhering in the artery per microscope field (×100) and expressed the results as the number of leukocytes observed per mm^2 area per minute.

Statistical analysis. Data are presented as means ± SEM. Comparison of two groups was analyzed by Student's *t* test. For comparison of more than two groups with comparable variances, one-way ANOVA was performed, followed by Tukey's *t* test to evaluate pair-wise group differences. An associated probability (*P* value) of less than 0.05 was considered significant. Analyses were performed with the use of GraphPad Software Prism 3.0.

Acknowledgments

We are grateful to H. Wise for helpful discussions; K. Deguchi, T. Fujiwara, and N. Kitagawa for animal care and breeding; and T. Arai, H. Nose, and Y. Kitagawa for secretarial assistance. This work was supported in part by Grants-in-Aid for Scientific Research from the Ministry of Education, Science, Sports and Culture of Japan and by grants from the Organization for Pharmaceutical Safety and Research and the Kowa Life Science Foundation.

Received for publication March 1, 2004, and accepted in revised form July 27, 2004.

Address correspondence to: Shuh Narumiya, Department of Pharmacology, Kyoto University Faculty of Medicine, Yoshida, Sakyo-ku, Kyoto 606-8501, Japan. Phone: +81-75-753-4392; Fax: +81-75-753-4693; E-mail: snaru@mfour.med.kyoto-u.ac.jp.

1. Ross, R. 1999. Atherosclerosis is an inflammatory disease. *Am. Heart. J.* 138:S419–S420.
2. FitzGerald, G.A., Smith, B., Pedersen, A.K., and Brash, A.R. 1984. Increased prostacyclin biosynthesis in patients with severe atherosclerosis and platelet activation. *N. Engl. J. Med.* 310:1065–1068.
3. Belton, O., Byrne, D., Kearney, D., Leahy, A., and Fitzgerald, D.J. 2000. Cyclooxygenase-1 and -2-dependent prostacyclin formation in patients with atherosclerosis. *Circulation.* 102:840–845.
4. Plump, A.S., et al. 1992. Severe hypercholesterolemia and atherosclerosis in apolipoprotein E-deficient mice created by homologous recombination in ES cells. *Cell.* 71:343–353.
5. Zhang, S.H., Reddick, R.L., Piedrahita, J.A., and Maeda, N. 1992. Spontaneous hypercholesterolemia and arterial lesions in mice lacking apolipoprotein E. *Science.* 258:468–471.
6. Ishibashi, S., et al. 1993. Hypercholesterolemia in low density lipoprotein receptor knockout mice and its reversal by adenovirus-mediated gene delivery. *J. Clin. Invest.* 92:883–893.
7. Cyrus, T., et al. 2002. Effect of low-dose aspirin on vascular inflammation, plaque stability, and atherogenesis in low-density lipoprotein receptor-deficient mice. *Circulation.* 106:1282–1287.
8. Cayatte, A.J., et al. 2000. The thromboxane receptor antagonist S18886 but not aspirin inhibits atherogenesis in apo E-deficient mice: evidence that eicosanoids other than thromboxane contribute to atherosclerosis. *Arterioscler. Thromb. Vasc. Biol.* 20:1724–1728.
9. Vane, J.R., Bakhle, Y.S., and Botting, R.M. 1998. Cyclooxygenases 1 and 2. *Ann. Rev. Pharmacol. Toxicol.* 38:97–120.
10. McAdam, B.F., et al. 1999. Systemic biosynthesis of prostacyclin by cyclooxygenase (COX)-2: the human pharmacology of a selective inhibitor of COX-2. *Proc. Natl. Acad. Sci. U. S. A.* 96:272–277.
11. Topper, J.N., Cai, J., Falb, D., and Gimbrone, M.A., Jr. 1996. Identification of vascular endothelial genes differentially responsive to fluid mechanical stimuli: cyclooxygenase-2, manganese superoxide dismutase, and endothelial cell nitric oxide synthase are selectively up-regulated by steady laminar shear stress. *Proc. Natl. Acad. Sci. U. S. A.* 93:10417–10422.
12. Foeldvari, I. 2002. A selective COX-2 inhibitor, meloxicam, as a treatment option in patients with juvenile idiopathic arthritis and gastrointestinal side effects from naproxen [letter]. *Clin. Exp. Rheumatol.* 20:874.
13. Mukherjee, D., Nissen, S.E., and Topol, E.J. 2001. Risk of cardiovascular events associated with selective COX-2 inhibitors. *JAMA.* 286:954–959.
14. Rott, D., et al. 2003. Effects of MF-tricyclic, a selective cyclooxygenase-2 inhibitor, on atherosclerosis progression and susceptibility to cytomegalovirus replication in apolipoprotein-E knockout mice. *J. Am. Coll. Cardiol.* 41:1812–1819.
15. Burleigh, M.E., et al. 2002. Cyclooxygenase-2 promotes early atherosclerotic lesion formation in LDL receptor-deficient mice. *Circulation.* 105:1816–1823.
16. Pratico, D., Tillmann, C., Zhang, Z.B., Li, H., and FitzGerald, G.A. 2001. Acceleration of atherogenesis by COX-1-dependent prostanoid formation in low density lipoprotein receptor knockout mice. *Proc. Natl. Acad. Sci. U. S. A.* 98:3358–3363.
17. Belton, O.A., Duffy, A., Toomey, S., and Fitzgerald, D.J. 2003. Cyclooxygenase isoforms and platelet vessel wall interactions in the apolipoprotein E knockout mouse model of atherosclerosis. *Circulation.* 108:3017–3023.
18. Narumiya, S., Sugimoto, Y., and Ushikubi, F. 1999. Prostanoid receptors: structures, properties, and functions. *Physiol. Rev.* 79:1193–1226.
19. Kabashima, K., et al. 2003. Thromboxane A_2 modulates interaction of dendritic cells and T cells and regulates acquired immunity. *Nat. Immunol.* 4:694–701.
20. Murata, T., et al. 1997. Altered pain perception and inflammatory response in mice lacking